Accepted Manuscript

Structural insights of cyclin dependent kinases: Implications in design of selective inhibitors

Sourav Kalra, Gaurav Joshi, Anjana Munshi, Raj Kumar

PII: S0223-5234(17)30682-7

DOI: 10.1016/j.ejmech.2017.08.071

Reference: EJMECH 9715

To appear in: *European Journal of Medicinal Chemistry*

Received Date: 19 March 2017

Revised Date: 31 August 2017

Accepted Date: 31 August 2017

Please cite this article as: S. Kalra, G. Joshi, A. Munshi, R. Kumar, Structural insights of cyclin dependent kinases: Implications in design of selective inhibitors, *European Journal of Medicinal Chemistry* (2017), doi: 10.1016/j.ejmech.2017.08.071.

This is a PDF file of an unedited manuscript that has been accepted for publication. As a service to our customers we are providing this early version of the manuscript. The manuscript will undergo copyediting, typesetting, and review of the resulting proof before it is published in its final form. Please note that during the production process errors may be discovered which could affect the content, and all legal disclaimers that apply to the journal pertain.

Structural Insights of Cyclin Dependent Kinases: Implications in Design of Selective Inhibitors

Sourav Kalra[1], Gaurav Joshi[2], Anjana Munshi[1], Raj Kumar[2]*

[1] *Centre for Human Genetics and Molecular Medicine, School of Health Sciences,*[2] *Centre for Pharmaceutical Sciences and Natural Products, School of Basic and Applied Sciences.*

Central University of Punjab, Bathinda

E-mail: raj.khunger@gmail.com, rajcps@cup.ac.in; Tel: +91-0164-2864215; fax: +91-1636-236564

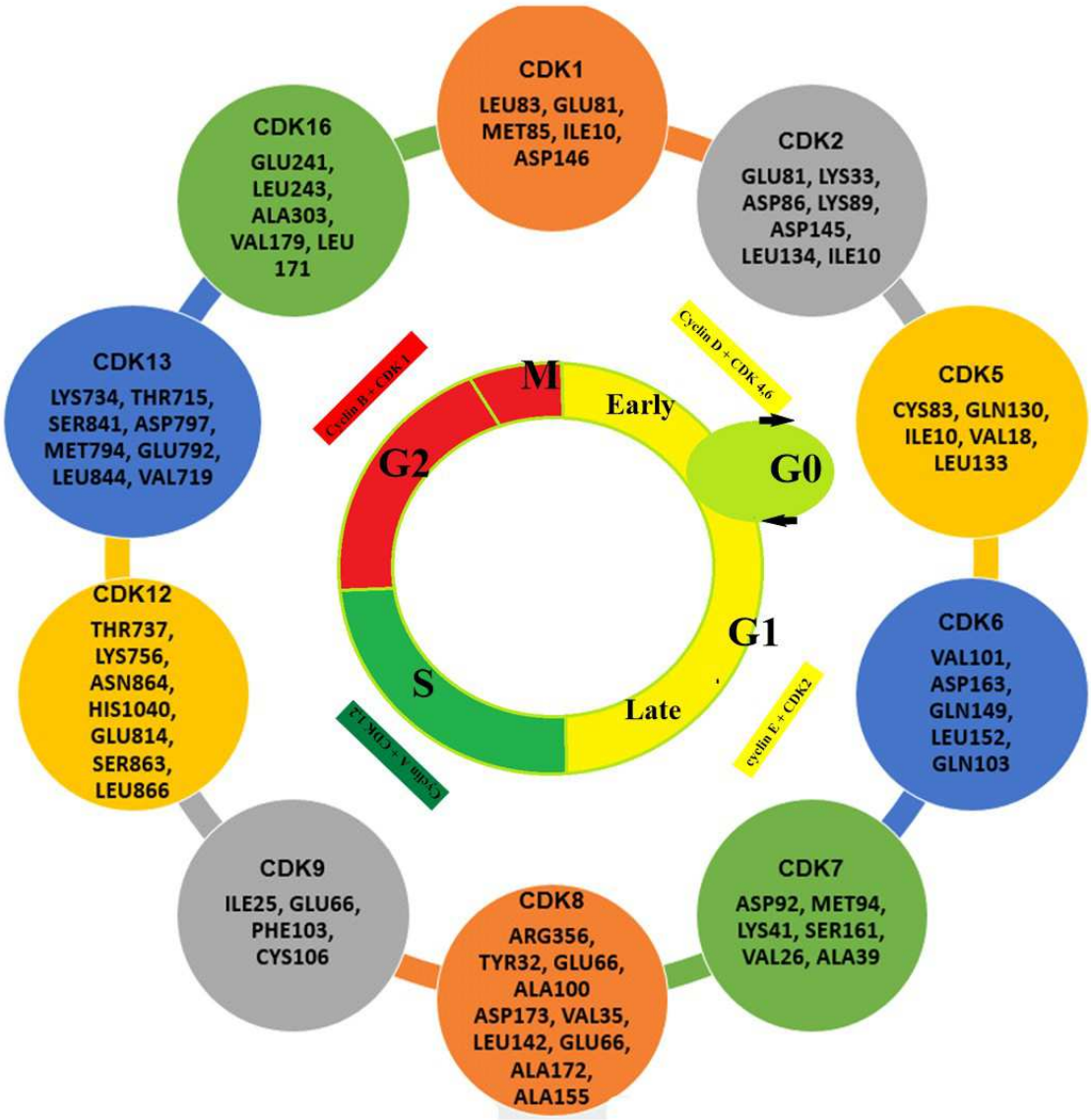

ACCEPTED MANUSCRIPT

Structural Insights of Cyclin Dependent Kinases: Implications in Design of Selective Inhibitors

Sourav Kalra[1], Gaurav Joshi[2], Anjana Munshi[1*], Raj Kumar[2]**

[1] *Centre for Human Genetics and Molecular Medicine, School of Health Sciences,*[2] *Centre for Pharmaceutical Sciences and Natural Products, School of Basic and Applied Sciences, Central University of Punjab, Bathinda.*

[**]Corresponding author: E-mail: raj.khunger@gmail.com, rajcps@cup.ac.in; Tel: +91-0164-2864215; fax: +91-1636-236564; *Co-corresponding author: E-mail: anjanadurani@yahoo.co.in

Abstract

There are around 20 Cyclin-dependent kinases (CDKs) known till date, and various research groups have reported their role in different types of cancer. The X-ray structures of some CDKs especially CDK2 was exploited in the past few years, and several inhibitors have been found, e.g., flavopiridol, indirubicin, roscovitine, etc., but due to the specificity issues of these inhibitors (binding to all CDKs), these were called as pan inhibitors. The revolutionary outcome of palbociclib in 2015 as CDK4/6 inhibitor added a new charm to the specific inhibitor design for CDKs. Computer-aided drug design (CADD) tools added a benefit to the design and development of new CDK inhibitors by studying the binding pattern of the inhibitors to the ATP binding domain of CDKs. Herein, we have attempted a comparative analysis of structural differences between several CDKs ATP binding sites and their inhibitor specificity by depicting the important ligand- receptor interactions for a particular CDK to be targeted. This perspective provides futuristic implications in the design of inhibitors considering the spatial features and structural insights of the specific CDK.

Keywords: cyclin dependent kinases, cyclins, CDK inhibitors, drug design, cancer

ACCEPTED MANUSCRIPT

Highlights

- CDKs are involved in cell cycle progression, and many of them are overexpressed in various cancers
- Development of a specific CDK inhibitor is a challenge and requires exploitation of X-ray structures
- Nature and position of active site residues, ligand-CDK binding and structural features of ligand play a major role in the design of selective CDK inhibitors

ACCEPTED MANUSCRIPT

1. Introduction

Cell cycle dysregulation resulting in mitogenic signaling and leading to uncontrolled proliferation is one of the hallmarks of cancer [1-4]. Cyclin-dependent kinases (CDKs), a family of serine/threonine protein kinases are known to play a vital role in cell cycle regulation and modulate transcription activity [5, 6]. Unlike other kinases, CDKs require cyclin (a protein subunit) that provides additional sequences for enzymatic activity [7]. Till date, 20 subfamilies of CDKs are known; three (CDK1, 4 and 5) are involved in cell cycle, and five (CDK 7, 8, 9 and 11) are associated with transcription [8-10]. In brief, all the CDKs have a two-lobed structure-N-terminal having beta sheets and C-terminal composed of α-helices. N-terminal lobe contains G-loop (rich in glycine) inhibitory component, and C-terminal contains activation segment that also includes phosphorylation residues; serine or threonine (known as T-loop in the case of CDKs) (Figure 1).

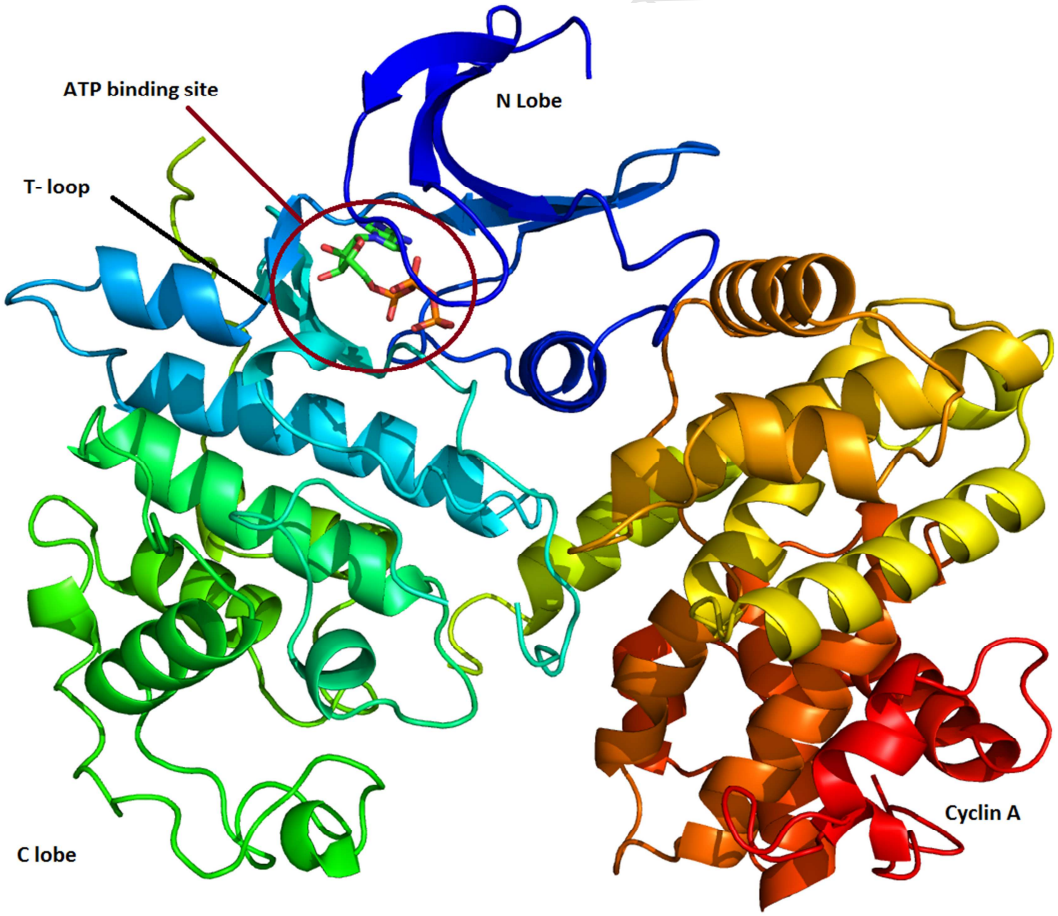

Figure 1. Representation of CDK2 as a prototype CDK protein bound with cyclin A and ATP and T loop helps in activation of the ATP binding site when cyclin gets bound to the CDK

Table 1. Cyclin dependent kinases: classification, their role, and association in cancer

CDK subtypes	Biological role	Cyclin partner	Role in type of cancer	Location on chromosome	Crystal structure available
CDK1	Control of M phase of cell cycle [11]	Cyclin B	Breast cancer, Lung cancer, Bladder cancer	10q21.2 13.80 kbp	Yes
CDK2	Control of G1-S phase of cell cycle [12]	Cyclin E	Breast Cancer, Melanoma	12q13.2 4.6 kbp	Yes
CDK2	Control of G1-S phase of cell cycle [12]	Cyclin A	Thymic Carcinoma, Lymphoma	12q13.2 4.6 kbp	Yes
CDK3	DNA damage Repair [13]	Cyclin C	Renal cancer, Lung cancer, Liver cancer	17q25.1 4.0 kbp	No
CDK4	Control of G1 phase of cell cycle and Rb/E2F transcription [14]	Cyclin D	Melanoma, Breast Cancer, Osteosarcoma, Skin cancer, Bladder cancer, Lung cancer	12q14.1 3.2kbp	Yes
CDK5	Neuronal function [15]	p35 and p39	Lung cancer, Neuroblastoma	7q36.1 3.8 kbp	Yes
CDK6	Control of G1 phase of cell cycle and Rb/E2F transcription [14]	Cyclin D	Breast cancer, Skin cancer, Bladder cancer, Stomach cancer	7q21.2 218 kbp	Yes
CDK7	Activates CDKs kinase, Involved in transcription	Cyclin H	Breast cancer, Lung cancer	5q13.2 42.1 kbp	Yes

	[16]				
CDK8	Role in Wnt/β-catenin pathway and RNAPII transcription [17, 18]	Cyclin C	-----	13q12.13 149.5 kbp	Yes
CDK9	RNAPII transcription and repair DNA damage [19]	Cyclin T	Breast cancer, Lung cancer, Cervical cancer	9q34.11 3.4 kbp	Yes
CDK10	ETS2 transcription [20]	Cyclin M	-----	16q24.3 24.3 kbp	No
CDK11A	RNA splicing [21]	Cyclin L	Urothelial cancer, Colorectal cancer, Head and Neck Cancer	1p36.33 24.61 kbp	No
CDK11B	RNA splicing [21]	Cyclin L	Urothelial cancer, Colorectal cancer, Head and Neck Cancer	1p36.33 24.61 kbp	No
CDK12	RNAPII transcription and DNA damage [22]	Cyclin K	Skin cancer, Pancreatic cancer, Melanoma, Lymphoma, Head and Neck Cancer, Cervical Cancer, Carcinoid	17q12 69.2 kbp	Yes
CDK13	RNAPII transcription [22, 23]	Cyclin K	Carcinoid, Colorectal cancer	7p14.1 144.1 kbp	Yes
CDK14	Role in Wnt/β-catenin pathway [24]	Cyclin Y	Prostate cancer	7q21.13 391.6 kbp	No
CDK15	Antiapoptotic protein[25]	Cyclin Y	Renal cancer, Pancreatic cancer	2q33.1 81.8 kbp	No

CDK16	Spermatogenesis [26]	Cyclin Y	Endometrial cancer, Lymphoma, Ovarian cancer	Xp11.3 5.2 kbp	Yes
CDK17	Phosphorylation of Histone protein [27]	--------	Carcinoid, Colorectal cancer, Melanoma, Renal cancer, Thyroid cancer	12q23.1 122.3 kbp	No
CDK18	Signal transduction cascade [28]	--------	Melanoma, Thyroid cancer, Cervical cancer, Glioma	1q32.1 8.1 kbp	No
CDK19	Transcriptional activity [18]	--------	Head and Neck cancer, Melanoma, Glioma, Prostrate cancer	6q21 131.1 kbp	No
CDK20	Activates CDK2[29].	--------	--------	9q22.1 6.9 kbp	No

The role of various CDKs in the cell cycle progression is represented in Figure 2. Briefly, p53 which is an important regulator of both G1/S, and G2/M checkpoint interacts with cyclin B and CDK1 [30]. After that cell enters early G1 phase, which is mitogen dependent and acted upon by cyclin D in conjugation with CDK 4 and 6 [31]. The growth factors are required to play their role at this point. Once the cell progress pasts the restriction point, mitogens are no longer needed for cell cycle progression. Cyclin D in conjugation with CDK4 and 6 promotes and ensures the cell progression beyond the limit point by phosphorylating and thus inhibiting retinoblastoma (RB), which allows E2F-mediated S-phase gene transcription[32, 33]. The cell then enters S-phase where DNA replication occurs. The G1/S checkpoint allows checking of DNA integrity before cell DNA is replicated. Cyclin A and CDK1, 2 play a vital role in S phase. CDK inhibitors thereby halt the progression of the cell cycle by inhibiting the cyclins and the CDKs. They act at multiple phases of cell cycle primarily at G1/S and G2/M checkpoints.

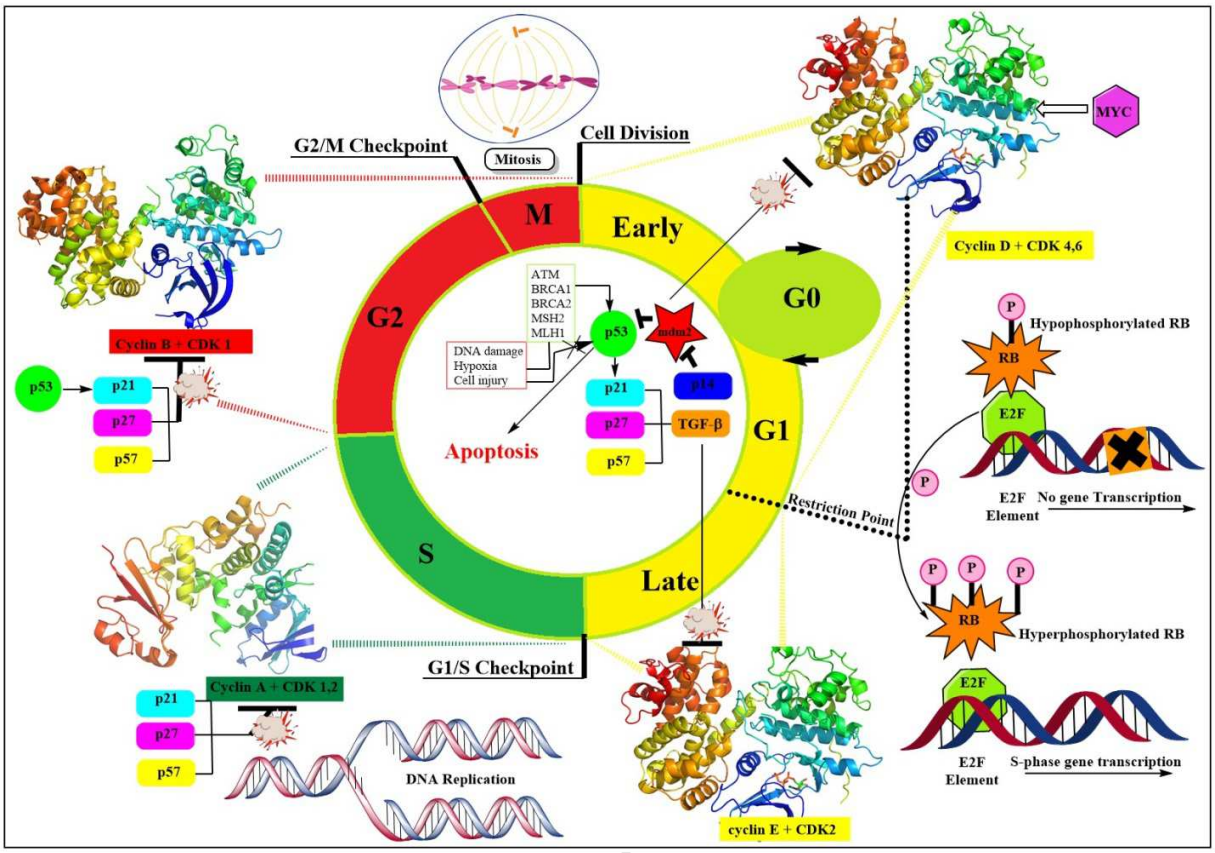

Figure 2. Illustrative view of cell cycle along with CDKs involved in cell cycle progression. The figure briefly explains the interaction of various oncogenes (cyclins, CDKs, E2F, MYC, Mdm2) and tumor suppressor (RB, p53, p21, p27, p57, p14, TGF-β, BRCA 1, BRCA 2, ATM) involved in cell cycle progression with CDKs.

Activation of CDK involves binding of CDKs with their respective cyclins at the C-terminal via noncovalent interactions and leads to the accessibility of ATP to the catalytic site for phosphorylation of threonine. A list depicting the association of cyclins with CDKs and their overexpression in various cancers has been presented in Table 1. Some of the CDKs do not require cyclin for activation; for instances, such as viral cyclins (cyclins from a virus), CDK5 activators (p35 and p39 have no homology with cyclins), RINGO/ Speedy family (small proteins with no homology to cyclins) [34, 35].

The endogenous ligands that activate the CDKs are mainly cyclins. These are classified as cyclin A, cyclin B, cyclin C, cyclin D, cyclin E, cyclin F, cyclin H, cyclin K, cyclin L and Cyclin T. These cyclins play a significant role in cell cycle progression by activation of ATP binding site.

Cyclin A forms a complex with CDK1 and CDK2 and helps in the regulation of S phase [11, 36]. Cyclin B is also called as maturation or mitosis promoting factor as it forms complex with CDK1 and controls the M phase of the cell cycle [11, 36]. Cyclin C and H activate CDK8 which in turn plays a significant role in RNAPII transcription and also inhibits the lipogenesis [17, 37]. Cyclin D in complex with CDK4 and CDK6 controls the G1 phase of cell cycle [38]. Cyclin E helps in the Rb/E2F transcription via formation of a complex with the CDK2 and controls G1-S phase [39]. Cyclin K helps in the RNAPII transcription by forming a complex with CDK12 and CDK13 [22, 23, 40]. Cyclin L and CDK11 associate to perform RNA splicing. Cyclin T with CDK9 plays a major role in RNAPII transcription [41]. Cyclin Y/CDK14 drives the Wnt/β-catenin pathway [42].

The cyclin-dependent kinase deactivation is carried out by a particular group of proteins cyclin-dependent kinase inhibitors (CDKIs). These group of proteins blocks kinase activity by interfering with the interaction of cyclin-CDK complex [43]. The inhibition of CDK naturally occurs during a G1 phase in response to signals from damaged DNA. In the eukaryotic cells, there are two types of naturally occurring (CDKIs) families namely the INK4 (inhibitor of CDK4/6) family and the CIP/KIP (inhibit other CDKs) [44]. The INK4 family comprises of $p16^{INK4a}$, $p18^{INK4c}$, $p15^{INK4b}$, and $p19^{INK4}$ which are specific inhibitors of CDK4 and CDK6, that binds to the CDK monomers [45]. These proteins are also reported to play a major role in tumor suppression, aging, apoptosis and DNA repair [46]. CIP/KIP proteins are nonspecific and bind to cyclin and CDK or cyclin/CDK complex. This family of proteins enhances complex cyclin D-CDK4/6 formation by activation of cyclin D [43].

The dysregulated activation of CDKs has been associated with various cancers, viral infections [47, 48], Alzheimer [49], Parkinson [50, 51], renal diseases [52] and ischemia[47, 48]. The role of CDKs in the pathogenesis of various diseases has encouraged an intensive search for potent and selective pharmacological inhibitors of CDKs [53].

The inhibition of the CDKs occurs naturally by INK4s and CIPs. Small molecules are being discovered and developed as CDK inhibitors which mainly target ATP binding domain of CDK-cyclin complexes in a reversible and competitive manner or by allosteric inhibition (Figure 3) [54, 55]. Betzi et al. elucidated the structure of CDK2 with the inhibitor ANS that acts on allosteric site [56, 57]. In 2015, palbocicilib was approved by FDA as CDK4/6 inhibitor.

Recently, ribocicilib (Kisqali) and abemacicilib are approved by FDA in March and July 2017, respectively. Although several CDK inhibitors such as, selicicilib, micicilib, dinacicilib, AT7519, atuvecicilib, SNS-032, etc. are in various clinical phases and some (covalent inhibitors: THZ1, THZ531, and BS-181, LDC000067) are under preclinical development stage (Figure S3) but developing a potent and selective inhibitor is still a challenge (Figure 4)[58-61].

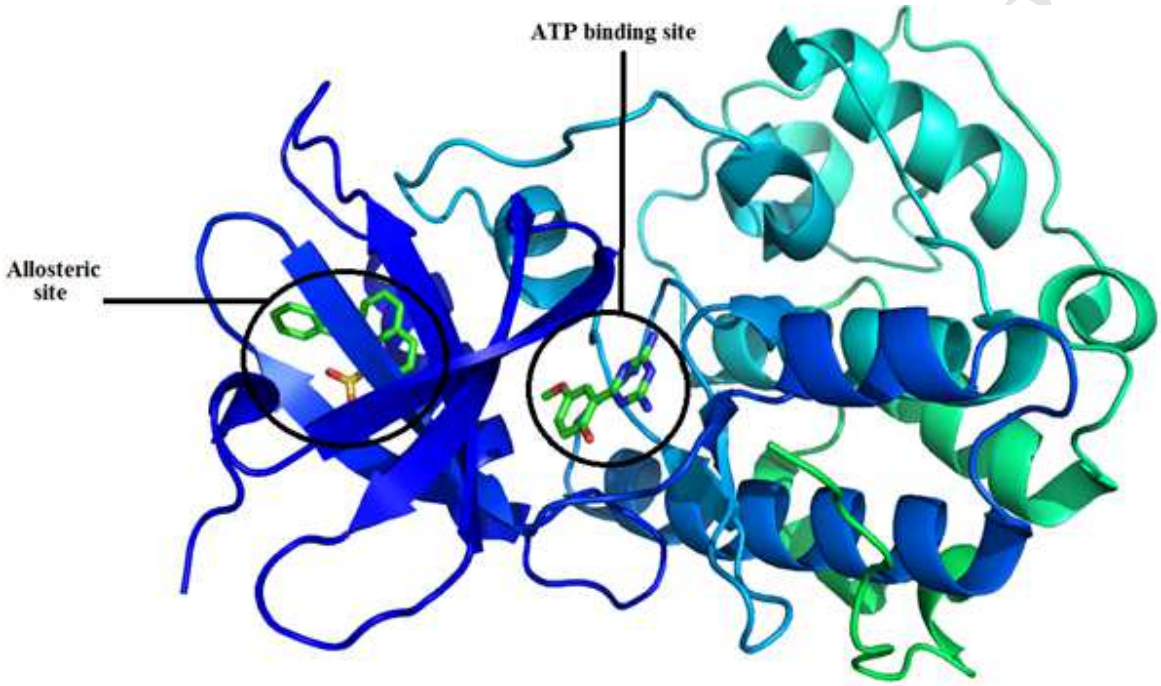

Figure 3. Structure depicting the Cyclin Dependent Kinase 2 with JWS648 inhibitor in ATP binding site and ANS in allosteric binding site (PDB ID: 3PXZ)

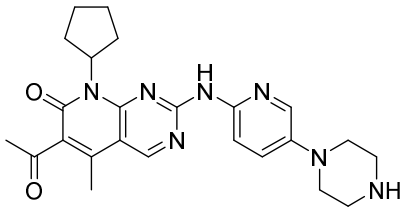

Palbocicilib
FDA approved CDK4/6 inhibitor
CDK4= 11nM
CDK6=16nM

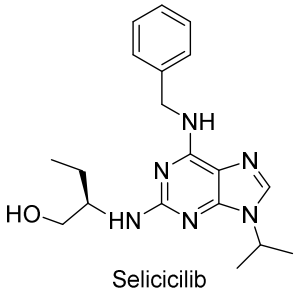

Selicicilib
Phase II
CDK2= 0.7uM
CDK5=0.16uM

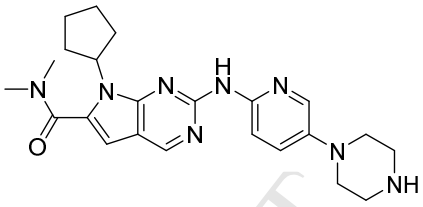

Ribocicilib
FDA approved CDK4/6 inhibitor
CDK4= 2nM
CDK6= 6nM

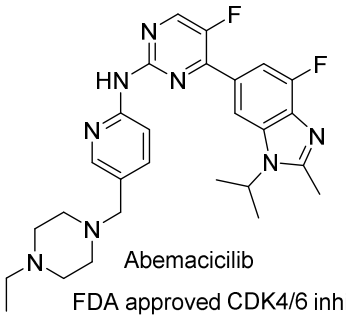

Abemacicilib
FDA approved CDK4/6 inhibitor
CDK4= 2nM
CDK6= 10nM

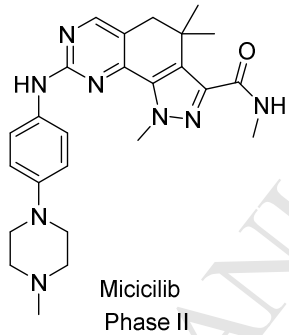

Micicilib
Phase II
CDK2= 45nM

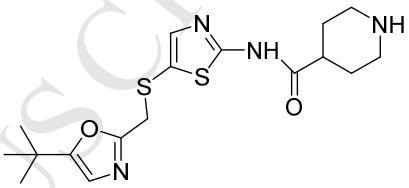

SNS-032
Phase I
CDK2= 48nM
CDK9= 4nM

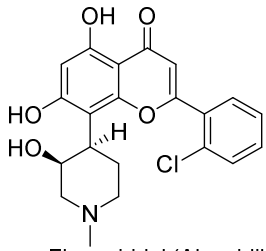

Flavopiridol (Alvocidib)
Phase I/II
CDK1= 30nM
CDK2= 170nM
CDK4= 100nM
CDK9= 20nM

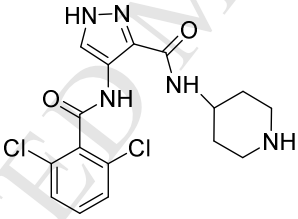

AT- 7519
Phase II
CDK2= 47nM
CDK9= 10nM

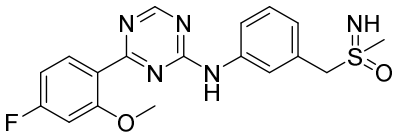

Phase I
Atuvecicilib
CDK9=385nM

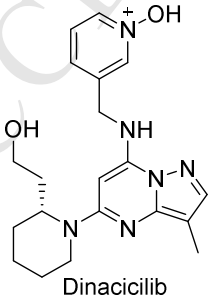

Dinacicilib
Phase II
CDK1= 3nM
CDK2= 1nM
CDK5= 1nM

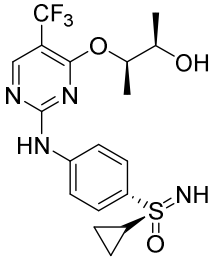

Ronicicilib
Phase II
CDK1= 7nM
CDK2= 9nM

ACCEPTED MANUSCRIPT

Figure 4. Chemical structures of CDK inhibitors along with their clinical status, selectivity and inhibitory concentrations.

A review by Roskoski covered CDK inhibitors in clinical and preclinical studies [54]. Recently Li et al. published a review article which mainly dealt with CDK inhibitors and their structure-activity relationship studies [55]. The present manuscript is first of its kind, its first part highlights on overview of each class of CDKs, their inhibitors, and their available X-ray crystal structures till date. The next section deals with factors contributing to the selective inhibition of a particular CDK based on either active site residues of CDK, ligand-CDK binding or chemical architecture of ligand, etc. The facts were further corroborated by taking case studies and performing computational studies.

2. CDKs: Location, X-ray structures, and sequence alignment

2.1.CDK1

CDK1 encoding for CDK1 protein is located on chromosome 10q21.2 13.80 kbp in length. The gene is ranging from 62,539,923 positions to 62,553,733 on the chromosome. Four crystal structures of CDK1 are known. All the PDB IDs have a similar number of residues except in 5HQ0 which represents the CDK1 protein as a dimer. It was observed that LEU83, GLU81 form hydrogen bond and MET85, ILE10, ASP146 possess hydrophobic interactions with CDK1 inhibitor LZ9 (Table 2; Figure 5)

Table 2. X-ray crystal structures of CDK1

PDB ID	Resolution (Å)	Total residues	Co-crystallized ligand	Ligand interactions with amino acids (if available)	Reference
4Y72	2.3	659	LZ9	LEU83, GLU81, MET85, ILE10, ASP146	[62]
4YC3	2.7	659	MPD (Pentanediol)	ASP146	
4YC6	2.6	654	No Ligand	--	
5HQ0	2.3	1528	LZ9	LEU83, GLU81, MET85, ILE10, ASP146	

CDK1 protein active site residues were aligned to CDK2 protein active site using Smith-Waterman Sequence Alignment as CDK2 is the more extensively studied CDK. It was observed that both the proteins had89.19 % similar residues and 74.32 % identical residues (Chart 1 and Figure 5d).

```
Query:      4Y72 Chain: A, Length: 302
Subject:    4FKL Chain: A, Length: 74
Identities: 55/82, i.e., 18.21 % (query) and 74.32 % (subject)
Similars:   66/82, i.e., 21.85 % (query) and 89.19 % (subject)

    4Y72.A  6 MEDYTKIEKIGEGTYGVVYKGRHKTTGQVVAMKKIRLESEEEGVPSTAIREISLLKELRH 65
              ||.. |.|||||||||||||| |.| ||.|||.|||        |||||||||||||| |
PDP:4FKLAa  1 MENFQKVEKIGEGTYGVVYKARNKLTGEVVALKKI--------VPSTAIREISLLKELNH 52
    4Y72.A 66 PNIVSLQDVLMQDSRLYLIFEF 87
              |||| | ||.  ...|||.|||
PDP:4FKLAa 53 PNIVKLLDVIHTENKLYLVFEF 74
Green - identical residues | Pink - similar residues | Blue - sequence mismatch | Brown –
insertion/deletion |
```

Chart 1. Smith Waterman sequence alignment depicting the sequence similarity and difference between the aligned protein CDK1 and CDK2

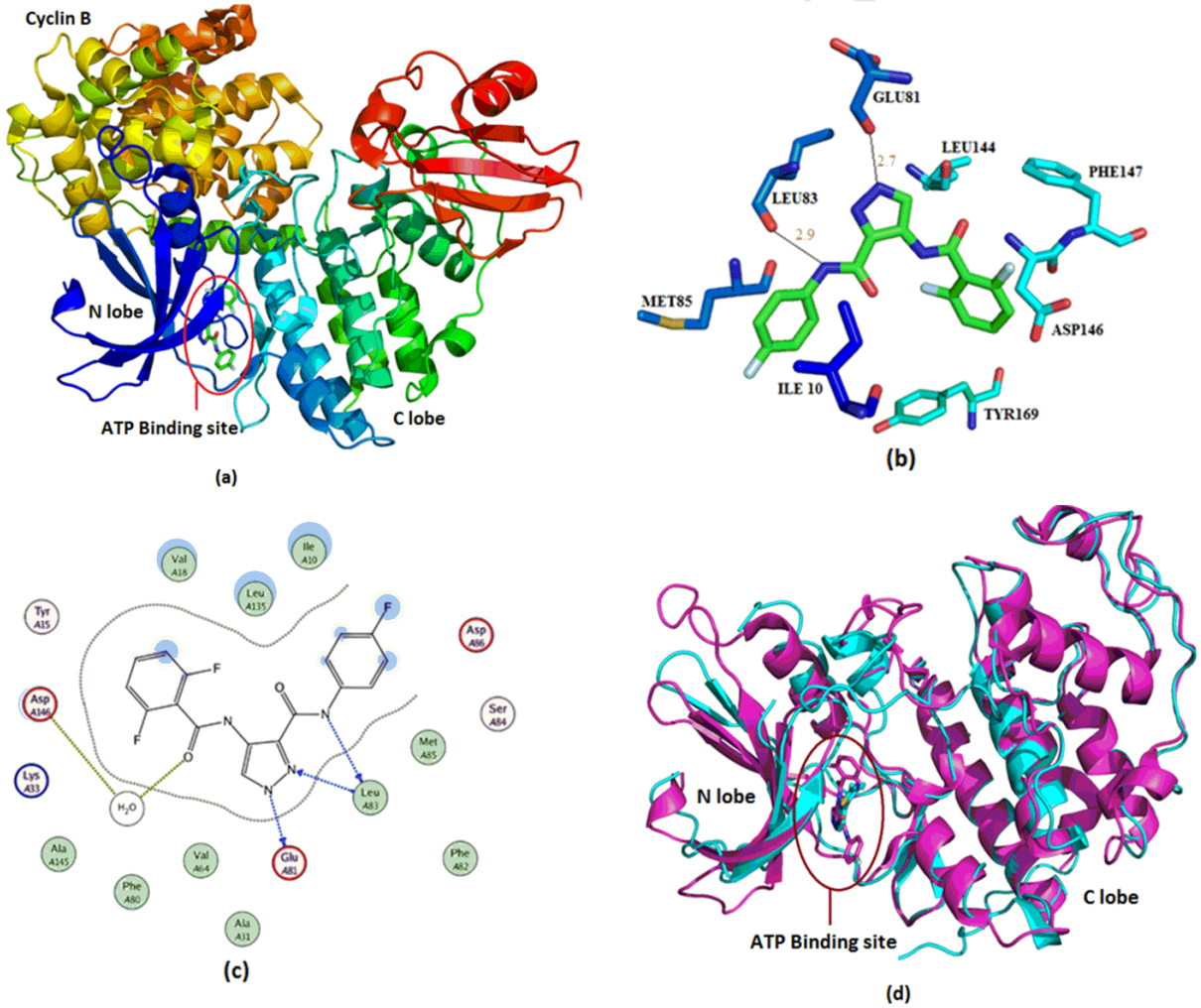

Figure 5. (a) 3D X-ray crystal structure of CDK1 with cyclin B (PDB ID: 4Y72) (b) 3D interaction diagram of bound inhibitor LZ9 in CDK1 active site (c) 2D interaction diagram

depicting critical amino acid residues for the inhibition of CDK1 (d) Aligned proteins showing the identical structures between the chains of CDK1 (Pink color) (PDB ID: 4Y72) and CDK2 (Cyan color) (PDB ID: 4FKL)

2.2. CDK2

CDK2 gene is located on the longer arm12q13.2. It is 4.6 kbp in length and occupies 56,360,792 positions to 56,365,409 on the chromosome. There are 800-900 crystal structures of CDK2 with ligands or inhibitors. Extensive work has been carried out to achieve inhibition of CDK2. All the PDB IDs have near about same residues, and some exist as dimers, trimers or tetramers. The monomeric CDK2 contains around 280-306 residues. In general, a CDK2 inhibitor binds to CDK2 via hydrogen bonding interactions (LEU 83, GLU 81), hydrophobic interactions (VAL18, ILE10, ASP146) and Pi-cation interactions (LYS33). Some of the selected PDB IDs of CDK2 with inhibitors/ligands and residues involved in interactions are summarized in Table 3; Table S1 see supplementary content and Figure 6 (b).

Table 3. X-ray crystal structures available for CDK2

PDB ID	**Resolution (Å)**	**Total residues**	**Co-crystallized ligand**	**Ligand interactions with amino acids (if available)**	**Reference**
4FKL	1.26	299	CK2	LYS33, GLU81, LEU134	
4II5	2.15	1112	ADP	LYS33, ASP86, LEU83, GLU81, GLN131, Mg^{++}, LEU134	[63]
5IEV	2.03	298	R0N	LEU83, ASP86, LEU134	[64]
5K4J	1.60	299	6QB	LEU83, ASN132, LEU134	[65]
5L2W	2.8	606	1QK (Dinacicilib)	LEU83, ILE10, PHE82, GLY11, VAL18. GLN131, ALA31, LEU134	[55]

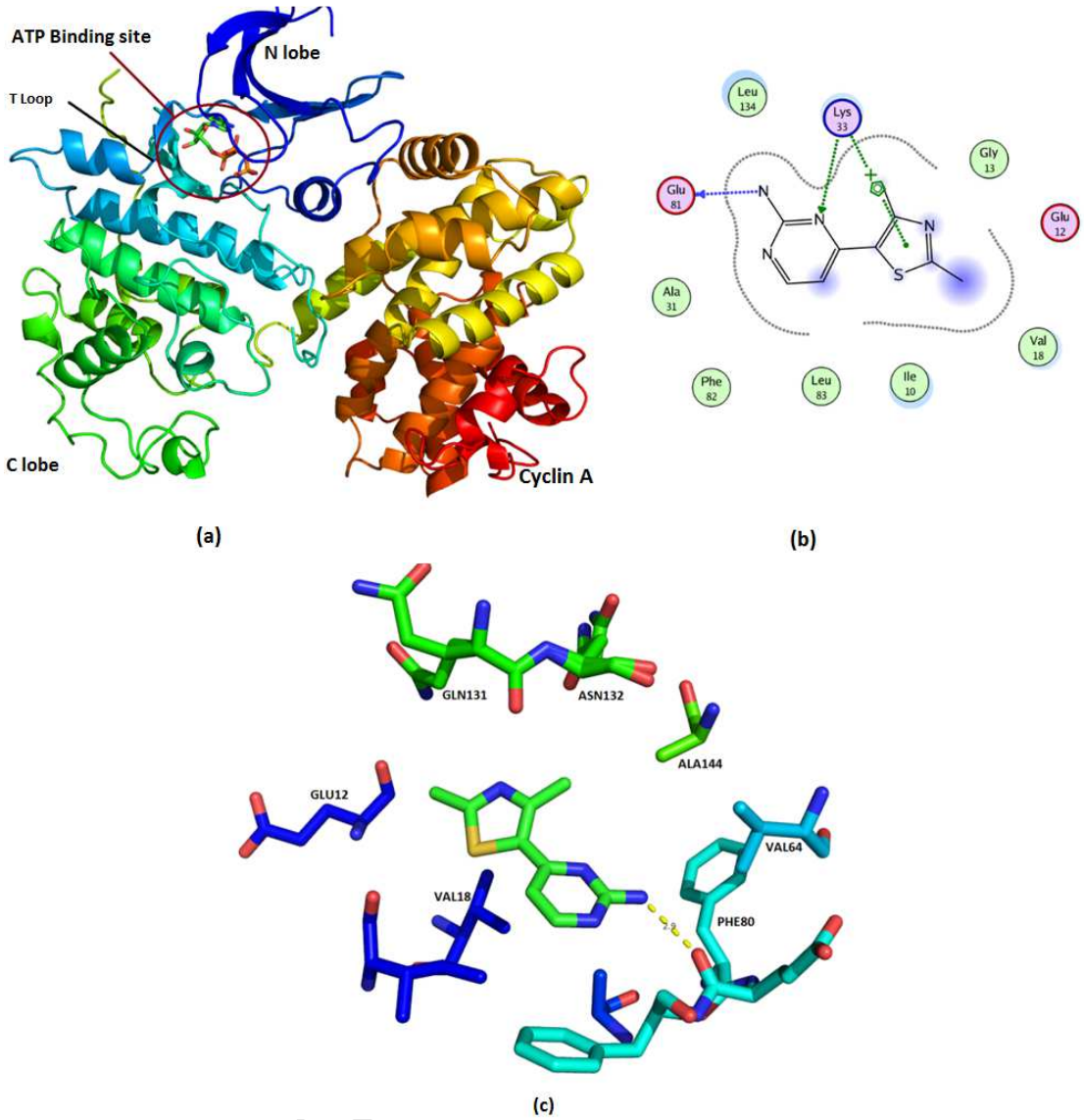

Figure 6. Structural features of Cyclin Dependent Kinase 2 (CDK2) (a) 3D X-ray crystal structure of protein PDB ID: 4FKL was taken as standard protein for comparison with other CDKs (b) 2D interaction diagram depicting the interaction of PDB ID: 4FKLwith inhibitor (c) 3D interaction diagram of bound inhibitor CK2in CDK2 active site

2.3.CDK4

Cyclin dependent kinase 4 is located on chromosome 12q14.1. It is a thin band of around 3.2 kbp ranges from 58,142,307 positions to 58,145,500 on the chromosome. Around five crystal structures of CDK4 have been reported without any co-crystallized ligand. All the PDB IDs have

similar 577 residues, except for dimer PDB ID: 3G33 contains 1228 residues (Table 4). The 3D crystal structure of CDK4 (PDB ID:2W9Z) has been represented in Figure 7(a)

Table 4. X-ray crystal structures for CDK4

PDB ID	Resolution (Å)	Total residues	Co-crystallized ligand	Reference
2W96	2.93	577	No ligand	[66]
2W99	2.8	577	No ligand	
2W9F	2.85	577	No ligand	
2W9Z	2.45	563	No ligand	
3G33	3.0	1228	No ligand	[67]

CDK4 protein active site residues were aligned to CDK2 protein active site. Both the proteins were having 70.27 % similar and 48.65 % identical residues (Chart 2 and Figure7b)

```
Query:      2W9Z Chain: B, Length: 306
Subject:    4FKL Chain: A, Length: 74
Identities: 36/86, i.e., 11.76 % (query) and 48.65 % (subject)
Similars:   52/86, i.e., 16.99 % (query) and 70.27 % (subject)

    2W9Z.B  6 YEPVAEIGVGAYGTVYKARDPHSGHFVALKSVRVPNGEEGLPISTVREVALLRRLEAFEH 65
              .. | .|| | || |||||.  .|  |||| .        .| . .||..||. |    |
PDP:4FKLAa  4 FQKVEKIGEGTYGVVYKARNKLTGEVVALKKI--------VPSTAIREISLLKELN---H 52

    2W9Z.B 66 PNVVRLMDVCATSRTDREIKVTLVFE 91
              ||.|.|.||  |     | |. ||||
PDP:4FKLAa 53 PNIVKLLDVIHT-----ENKLYLVFE 73
Legend: Green - identical residues | Pink - similar residues | Blue - sequence mismatch | Brown - insertion/deletion |
```

Chart 2. Smith Waterman sequence alignment depicting the sequence similarity and difference between the aligned protein CDK4 and CDK2

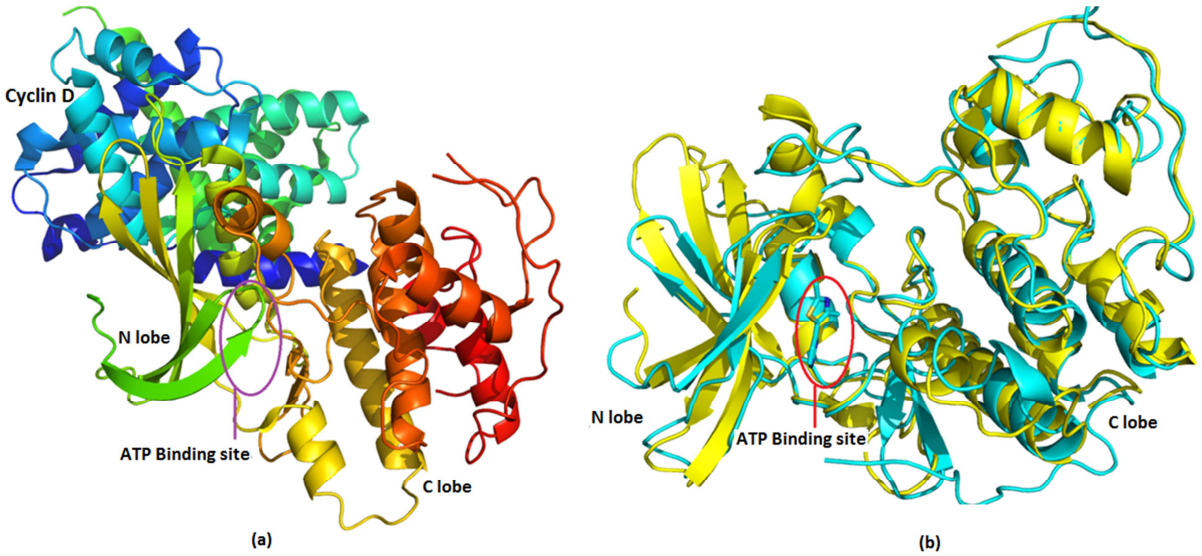

Figure 7. (a) 3D X-ray crystal structure of protein CDK4 (PDB ID: 2W9Z) (b) Aligned proteins showing the identical structures between the chains of protein CDK4 (yellow color) (PDB ID: 2W9Z) and CDK2 (cyan color) (PDB ID: 4FKL)

2.4. CDK5

CDK5 has appeared as an essential kinase in sensory pathways and is required for proper development of the brain. It is located on the long arm of chromosome 7. It positions 7q36 with 3.8 kbp size ranges from 150,751,095 position to 150,754,935 on the chromosome. There are six crystal structures of CDK5 known with good resolution, out of which 5 PDB IDs contain co-crystallized ligand and inhibitors while one PDB ID: 1H4L does not include any ligand. In general, the CDK 5 inhibitors interact with CDK5 via hydrogen bonding (CYS83, GLU 81), and hydrophobic interactions (ILE10, GLN85, and LEU133). The structure of some selected PDB IDs of CDK5 with inhibitors, ligands, and residues involved are depicted in Table 5, and the 3D and 2D interaction diagrams representing interactions of (PDB ID: 1UNH) with indirubicin are shown in Figure 8 (b) and (c).

Table 5. X-ray crystal structures available of CDK4

PDB ID	Resolution (Å)	Total residues	Co-crystallized ligand	Ligand interactions with amino acids (if available)	Reference
1H4L	2.65	877	No Ligand	--	[68]
1UNG	2.3	1000	ALH (ALOSINE)	CYS83, LEU133, ALA31	[69]
1UNH	2.35	1000	IXM	GLU81, CYS83,	

			(INDIRUBICIN)	ILE10, GLN85	
1UNL	2.2	1000	RRC (ROSCOVITINE)	CYS83, GLN130, ILE10, VAL18, LEU133	
3O0G	1.95	882	3O0	GLU81, CYS83	[70]
4AU8	1.9	592	Z3R	ILE10, ASP86, VAL18, ALA143, LEU133	[71]

The sequence alignment of CDK2 protein active site residues and CDK5 protein active site was carried out using Smith-Waterman Sequence Alignment. Both the proteins have shown 86.49% similar residues and 64.86 % identical residues (Chart 3 and Figure 8d).

```
Query:      1UNH chain: B, Length: 292
Subject:    4FKL Chain: A, Length: 74
Identities: 48/82, i.e., 16.44 % (query) and 64.86 % (subject)
Similars:   64/82, i.e., 21.92 % (query) and 86.49 % (subject)


    1UNH.B  1 MQKYEKLEKIGEGTYGTVFKAKNRETHEIVALKRVRLDDDDEGVPSSALREICLLKELKH 60
              |. ..|.|||||||||| |.||.|. | |.||||..        |||.|.||| ||||| |
PDP:4FKLAa  1 MENFQKVEKIGEGTYGVVYKARNKLTGEVVALKKI--------VPSTAIREISLLKELNH 52

    1UNH.B 61 KNIVRLHDVLHSDKKLTLVFEF 82
                |||.| ||.|.. || |||||
PDP:4FKLAa 53 PNIVKLLDVIHTENKLYLVFEF 74
Legend: Green - identical residues | Pink - similar residues | Blue - sequence mismatch | Brown - insertion/deletion |
```

Chart 3. Smith Waterman sequence alignment depicting the sequence similarity and difference between the aligned protein CDK5 and CDK2

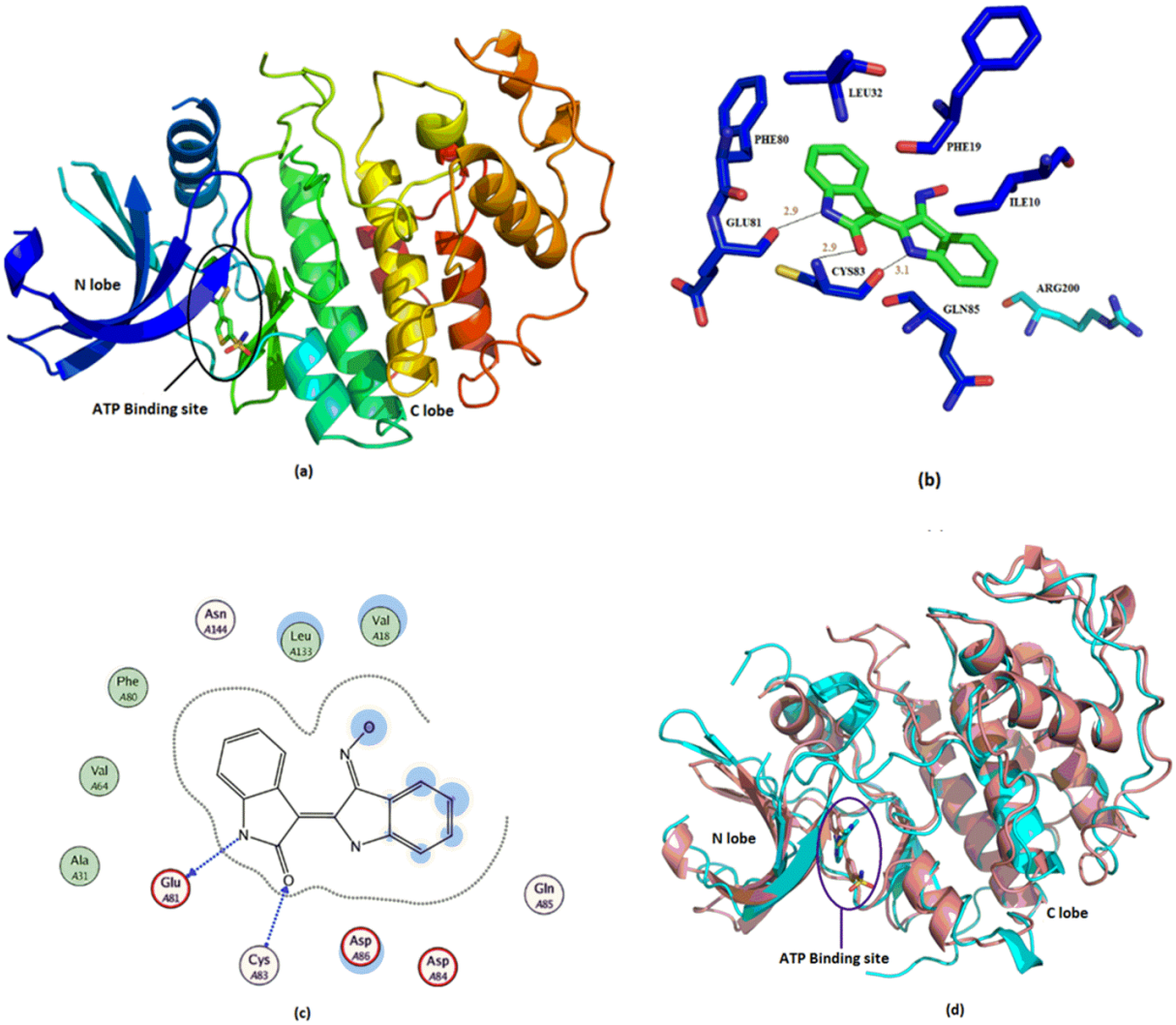

Figure 8. (a) 3D X-ray crystal structure of protein CDK5 (PDB ID: 1UNH) (b) 3D interaction diagram of bound inhibitor indirubicin in CDK5 active site (c) 2D interaction diagram depicting critical amino acid residues for the inhibition of CDK5 (d) Aligned proteins showing the identical structures between the chains of CDK5 (Peach color) (PDB ID: 1UNH) and CDK2 (cyan color) (PDB ID: 4FKL)

2.5. CDK6

CDK6 is regulated by cyclin D proteins. This gene is located on a longer arm of chromosome 7q21-22. There are 16 crystal structures of CDK6 known; only 11 contain co-crystallized ligands/inhibitors. Five of the sixteen PDB IDs known do not include any co-crystallized ligand. Generally, CDK6 protein (PDB ID: 2EUF) (Figure 9a) interacts with the inhibitors via hydrogen bonding (VAL101, ASP163) and hydrophobic interactions (LEU152, ILE19). The other

significant interactions for various PDB IDs of CDK6 are summarized in Table 6 and Table S2 (see supplementary content). The 3D and 2D interaction diagram representing interactions of CDK6 (2EUF) with palbocicilib are shown in Figure 9 (b) and (c).

Table 6. X-ray crystal structures of CDK6

PDB ID	Resolution (Å)	Total residues	Co-crystallized ligand	Ligand interactions with amino acids (if available)	Reference
1XO2	2.9	562	FSE (FIESTEIN)	LYS43, GLU61, PHE98, GLU99, ASP163, VAL101, ILE19, ILE19, LEU152, ALA162	[72]
2EUF	3.0	562	LQQ (Palbocicilib)	VAL101, ASP163, LEU152, ILE19	[73]
5L2T	2.37	307	6ZZ (Ribocicilib)	VAL101, ASP163, LEU152, ILE19, ALA41	[55]
5L2S	2.27	307	6ZV (Abemicicilib)	VAL101, LYS43, LEU152, ILE19	
5L2I	2.75	307	LQQ (Palbocicilib)	VAL101, ASP163, LEU152, ILE19	

The sequence alignment studies are done using Smith Waterman Sequence alignment in which the CDK6 protein was aligned to CDK2 protein. It was observed that both the proteins contain 71.62% similar residues and 50.00% identical residues (Chart 4 and Figure 9d).

```
Query:      2EUF Chain: A, Length: 307
Subject:    4FKL Chain: A, Length: 74
Identities: 37/89, i.e., 12.05 % (query) and 50.00 % (subject)
Similars:   53/89, i.e., 17.26 % (query) and 71.62 % (subject)

    2EUF.A 11 QQYECVAEIGEGAYGKVFKARDLKNGGRFVALKRVRVQTGEEGMPLSTIREVAVLRHLET 70
              . .. | .|||| || |.|||. |  |  ||||..        .| . |||...|. |
PDP:4FKLAa  2 ENFQKVEKIGEGTYGVVYKARN-KLTGEVVALKKI--------VPSTAIREISLLKELN- 51

    2EUF.A 71 FEHPNVVRLFDVCTVSRTDRETKLTLVFE 99
                |||.|.| ||        | || ||||
PDP:4FKLAa 51 --HPNIVKLLDVIHT-----ENKLYLVFE 73
Legend: Green - identical residues | Pink - similar residues | Blue - sequence mismatch | Brown - insertion/deletion |
```

Chart 4. Smith Waterman sequence alignment depicting the sequence similarity and difference between the aligned protein CDK6 and CDK2

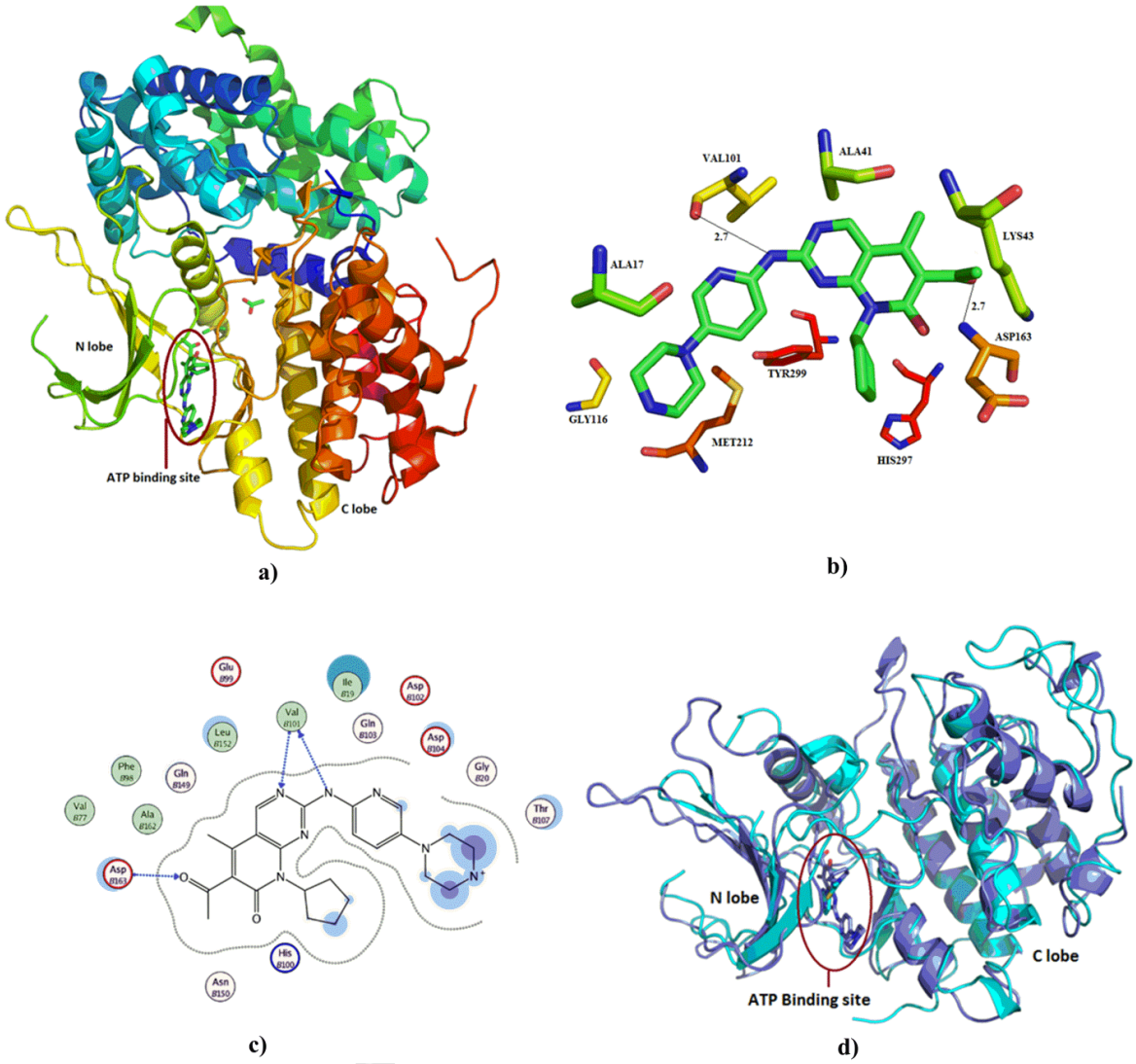

Figure 9. (a) 3D X-ray crystal structure of protein CDK6 (PDB ID: 2EUF) (b) 3D interaction diagram of bound inhibitor LQQ in CDK6 active site (c) 2D interaction diagram depicting critical amino acid residues for the inhibition of CDK6 (d) Aligned proteins showing the identical structures between the chains of CDK6 (purple color) (PDB ID: 2EUF) and CDK2 (cyan color) (PDB ID: 4FKL)

2.6. CDK7

CDK7 gene is located on chromosome 5q12.1. It is a thick band of around 42.1 kbp ranges from 68,530,802 positions to 68,572,962 on the chromosome. Only one crystal structure of CDK7 (PDB ID: 1UA2) has been reported (Figure 10a). It was observed that the ASP92, MET94,

LYS41, SER161 form hydrogen bonding and VAL26 and ALA39 possess hydrophobic interactions with the ATP (Table 7). The representation of interactions between CDK7 and ATP has been shown in Figure 10 (b) and (c)

Table 7. X-ray crystal structure of CDK7

PDB ID	Resolution (Å)	Total residues	Co-crystallized ligand	Ligand interactions with amino acids (if available)	Reference
1UA2	3.02	1384	ATP	ASP92, MET94, LYS41, SER161, VAL26, ALA39	[74]

Structural differences and similarity between CDK7 and CDK2 were calculated using the Smith-Waterman Sequence Alignment. It was observed that both the proteins were having 62.50 % similar residues and 45.83% identical residues and represented in Chart 5 and Figure 10(d).

```
Query:       1UA2 chain: , Length: 287
Subject:     4FKL chain: , Length: 216
Identities: 99/219, i.e., 34.49 % (query) and 45.83 % (subject)
Similars:   135/219, i.e., 47.04 % (query) and 62.50 % (subject)

   d1ua2a_  70 METDLEVIIKDNSLVLTP-SHIKAYMLMTLQGLEYLHQHWILHRDLKPNNLLLDENGVLK 128
               .  ||.  .  ..|   |   ||.|.   |||| . | |.|||||| |||..  | .|
PDP:4FKLAb   1 LHQDLKKFMDASALTGIPLPLIKSYLFQLLQGLAFCHSHRVLHRDLKPQNLLINTEGAIK  60

   d1ua2a_ 129 LADFGLAKSFGSPNRAYTHQVVTRWYRAPELLFGARMYGVGVDMWAVGCILAELLLRVPF 188
               |||||||..|| | | |||.||| ||||||.| | . |   ||.|..||| ||.. |
PDP:4FKLAb  61 LADFGLARAFGVPVRTYTHEVVTLWYRAPEILLGCKYYSTAVDIWSLGCIFAEMVTRRAL 120

   d1ua2a_ 189 LPGDSDLDQLTRIFETLGTPTEEQWPDMCSLPDYVTFKSFPGIPLHHIFSAA----GDDL 244
                ||||..||| ||| ||||| |  ||. |.|||    |||    .  ||       .|
PDP:4FKLAb 121 FPGDSEIDQLFRIFRTLGTPDEVVWPGVTSMPDYKP--SFPKWARQD-FSKVVPPLDEDG 177

   d1ua2a_ 245 LDLIQGLFLFNPCARITATQALKMKYFSNRPGPTPGCQL 283
                 |.  .  ..| ||.|  ||   .| .   | |  .|
PDP:4FKLAb 178 RSLLSQMLHYDPNKRISAKAALAHPFFQDVTKPVPHLRL 216
Legend: Green - identical residues | Pink - similar residues | Blue - sequence mismatch | Brown - insertion/deletion |
```

Chart 5. Smith Waterman Sequence Alignment depicting the sequence similarity and difference between the aligned protein CDK7 and CDK2

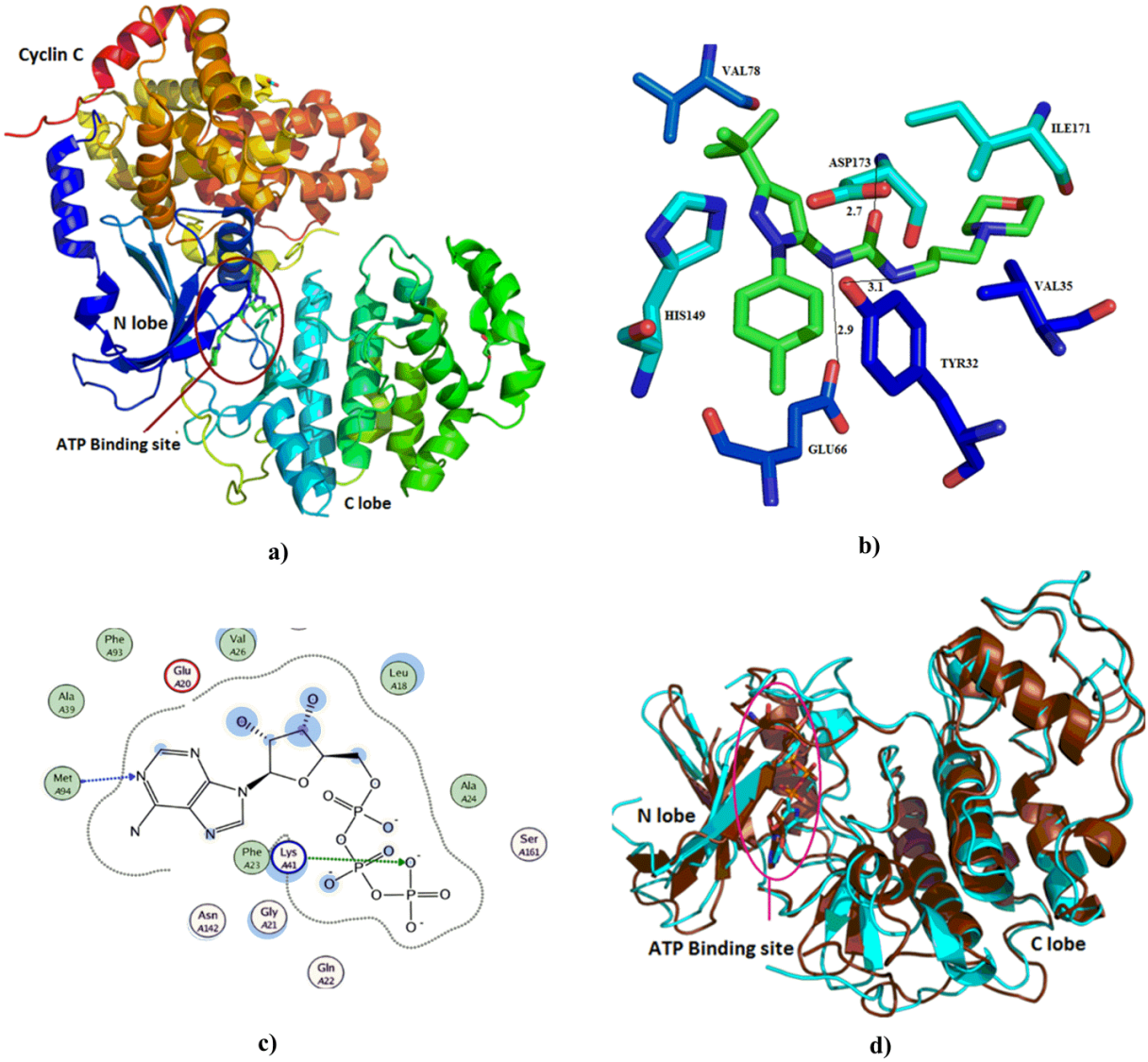

Figure 10. (a) 3D X-ray crystal structure of protein PDB ID: 1UA2) (b) 3D interaction diagram of ATP in CDK7 active site (c) 2D interaction diagram depicting critical amino acid residues in CDK7 (d) Aligned proteins showing the identical structures between the chains of CDK7 (Chocolate color) (PDB ID: 1UA2) and CDK2 (Cyan color) (PDB ID: 4FKL)

2.7. CDK8

CDK8 gene is located on chromosome 13q12.13. Twenty crystal structures of CDK8 are known containing the co-crystallized ligands. All the available crystal structures contain 690-692 residues. In general, all the CDK8 inhibitors interact with the CDK8 by the hydrogen bonding interactions (TYR32, GLU66, and ASP173) and hydrophobic interactions (GLU66 and

LEU132). The other significant interactions that are essential for CDK8 inhibition are summarized in Table 8 , Table S3 (see supplementary content) and Figure 11 (b) and (c)

Table 8. X-ray crystal structures of CDK8

PDB ID	Resolution (Å)	Total residues	Co-crystallized ligand	Ligand interactions with amino acids (if available)	Reference
3RGF	2.2	690	BAX	ALA100, PHE97, GLU166, PHE176, ASP173, ALA50, LEU158, MET174, ILE79, PHE97, ASP173	
4CRL	2.4	691	C1I	ALA100, VAL35, ALA50, LEU158	[75]
4F6S	2.6	692	0SQ	TYR32, GLU66, ASP173, LEU132, GLU66	[76]
4F6U	2.1	692	0SR	TYR32, GLU66, ASP173, LEU142, GLU66, TYR32, ALA50, LEU158, ILE79, PHE97	
4F6W	2.39	692	0SS	ARG356, TYR32, GLU66, ASP173, VAL35, LEU142, GLU66, ALA172, ALA155	

CDK8 protein was aligned to CDK2 protein using the Smith-Waterman Sequence Alignment. It was observed that both the proteins were having 57.41% similar residues and 38.43% identical residues. This has been represented in Chart 6 and Figure 11 (d).

```
Query:     4F6U chain: , Length: 233
Subject:   4FKL chain: , Length: 216
Identities: 83/225, i.e., 35.62 % (query) and 38.43 % (subject)
Similars:   124/225, i.e., 53.22 % (query) and 57.41 % (subject)

PDP:4F6UAa 10 KFHRASKVQ-LPRGMVKSLLYQILDGIHYLHANWVLHRDLKPANILVMGEGPERGRVKIA 68
              ||  || .  .|  ..|| |.|.| |. . |.. |||||||| |.|.  ||     .|.|
PDP:4FKLAb  7 KFMDASALTGIPLPLIKSYLFQLLQGLAFCHSHRVLHRDLKPQNLLINTEGA----IKLA 62

PDP:4F6UAa 69 DMGF--------------VVTFWYRAPELLLGARHYTKAIDIWAIGCIFAELLTSEPIFH 114
                | |               ||| |||||.||| ..|. |.|||..||||||..|   .|
PDP:4FKLAb 63 DFGLARAFGVPVRTYTHEVVTLWYRAPEILLGCKYYSTAVDIWSLGCIFAEMVTRRALFP 122

PDP:4F6UAa 115 CRQENPYHHDQLDRIFNVMGFPADKDWEDIKKMPEHSTLMKDFRRNTYTNCSLIKYMEKH 174
                   |     ||| |||  .| | .  |  .  ||..      . |  ..
```

```
PDP:4FKLAb 123 GDSEI----DQLFRIFRTLGTPDEVVWPGVTSMPDYKPSFPKWARQDFS---------- 167

PDP:4F6UAa 175 KVKP--DSKAFHLLQKLLTMDPIKRITSEQAMQDPYF--LEDPLP 215
                  || |  |     || ..|  || |||... |.  |.|  .  |.|
PDP:4FKLAb 168 KVVPPLDEDGRSLLSQMLHYDPNKRISAKAALAHPFFQDVTKPVP 212
```

Legend: *Green - identical residues | Pink - similar residues | Blue - sequence mismatch | Brown - insertion/deletion |*

Chart 6. Smith Waterman Sequence Alignment depicting the sequence similarity and difference between the aligned protein CDK8 and CDK2

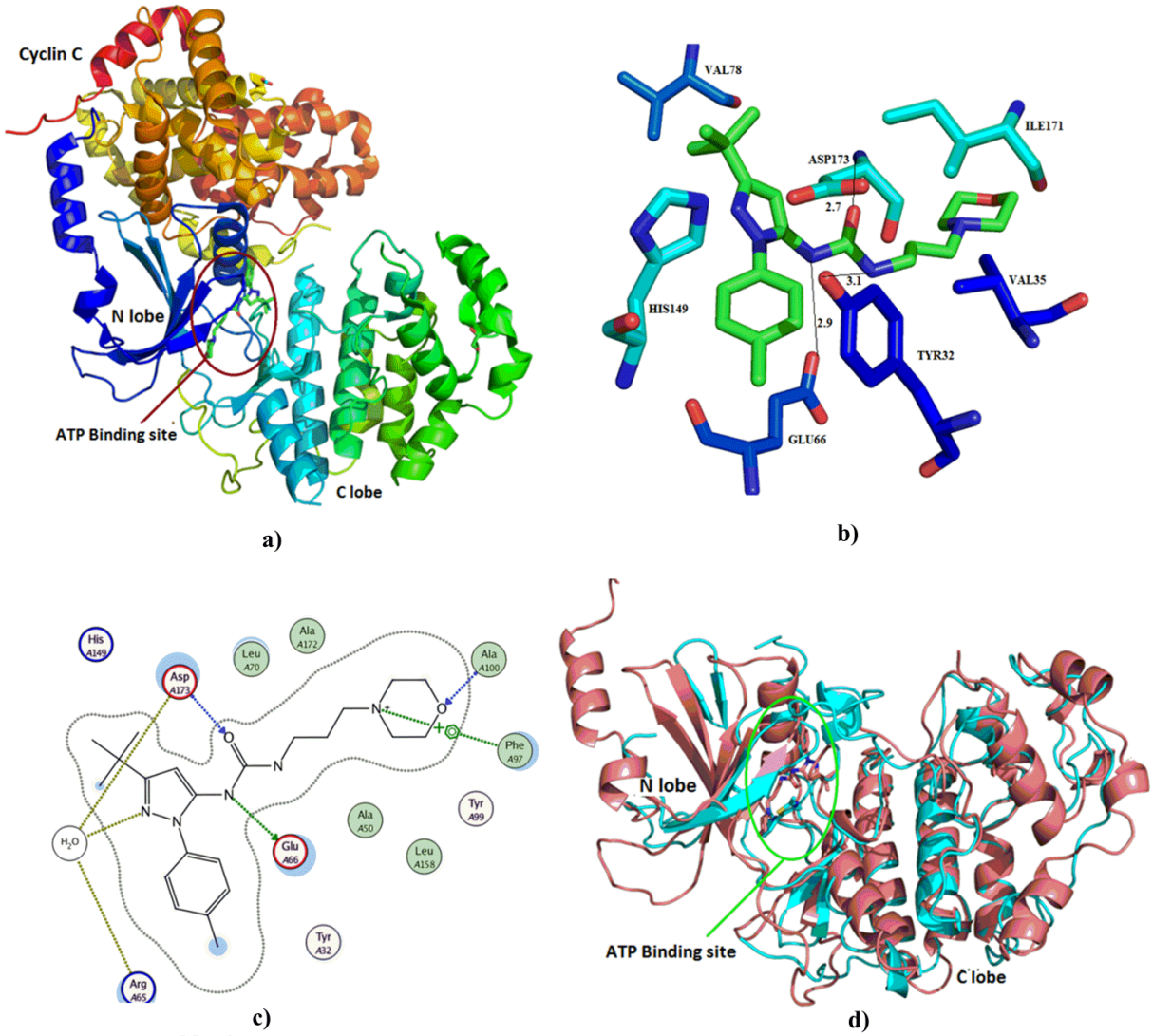

Figure 11. (a) 3D X-ray crystal structure of protein CDK8 (PDB ID: 4F6U) (b) 3D interaction diagram of bound inhibitor in CDK8 active site (c) 2D interaction diagram depicting critical amino acid residues for the inhibition of CDK8 (d) Aligned proteins showing the identical structures between the chains of CDK8 (dark peach color) ((PDB ID: 4F6U) and CDK2 (cyan color) (PDB ID: 4FKL)

2.8. CDK9

The CDK9 gene is positioned on chromosome 9q34.1. It ranges from 130,548,427 positions to 130,551,822 on the chromosome with a thin band of 3.4 kbp. 15 crystal structures of CDK9 are reported with ligands/inhibitors, except three. Generally, the CDK9 inhibitors bind to the CDK9 protein via hydrogen bonding interactions with CYS106, PHE30 and hydrophobic interactions with ILE25, LEU156. The other fundamental interactions of CDK9 inhibitors have been summarized in Table 9, Table S4 (see supplementary content) and Figure 12 (b) and (c).

Table 9. X-ray crystal structures of CDK9

PDB ID	Resolution (Å)	Total residues	Co-crystallized ligand	Ligand interactions with amino acids (if available)	Reference
3TNH	3.2	590	F18	ILE25, GLU66, PHE103, CYS106	[77]
3TN8	2.95	591	F18	ILE25, GLU66, PHE103, CYS106	
3MY1	2.80	591	RFZ	------	[78]
3BLR	2.80	591	CPB	CYS106, PHE30, ILE25, LEU156	[79]
3BLQ	2.90	591	ATP	LYS48, ASP104, CYS106, ASP167, ALA46	
3LQ5	3.0	591	SLQ	CYS106, PHE105, ILE25, LEU156, ALA46	[80]

A comparison of structural features between CDK9 and CDK2 was made by sequence alignment of CDK9 protein to CDK2 protein using Smith-Waterman Sequence Alignment. This similarity and the identical basis of the proteins were calculated, and the results have been depicted in Chart 7 and figure 12(d).

```
Query:      3BLR chain: A, Length: 331
Subject:    4FKL Chain: A, Length: 74
Identities: 37/90, i.e., 11.18 % (query) and 50.00 % (subject)
Similars:   60/90, i.e., 18.13 % (query) and 81.08 % (subject)

    3BLR.A 17 VSKYEKLAKIGQGTFGEVFKARHRKTGQKVALKKVLMENEKEGFPITALREIKILQLLKH 76
              .  ..|. |||.||.| |.|||.. ||. |||||..        | ||.||| .|. | |
PDP:4FKLAa  1 MENFQKVEKIGEGTYGVVYKARNKLTGEVVALKKIV--------PSTAIREISLLKELNH 52
```

```
    3BLR.A 77 ENVVNLIEICRTKASPYNRCKGSIYLVFDF106
                |.| |...  |.    |.    .||||.|
PDP:4FKLAa 53 PNIVKLLDVIHTE----NK----LYLVFEF 74
```

Legend: *Green - identical residues | Pink - similar residues | Blue - sequence mismatch | Brown - insertion/deletion |*

Chart 7. Smith-Waterman sequence alignment illustrating the sequence similarity and difference between the aligned protein CDK9 and CDK2

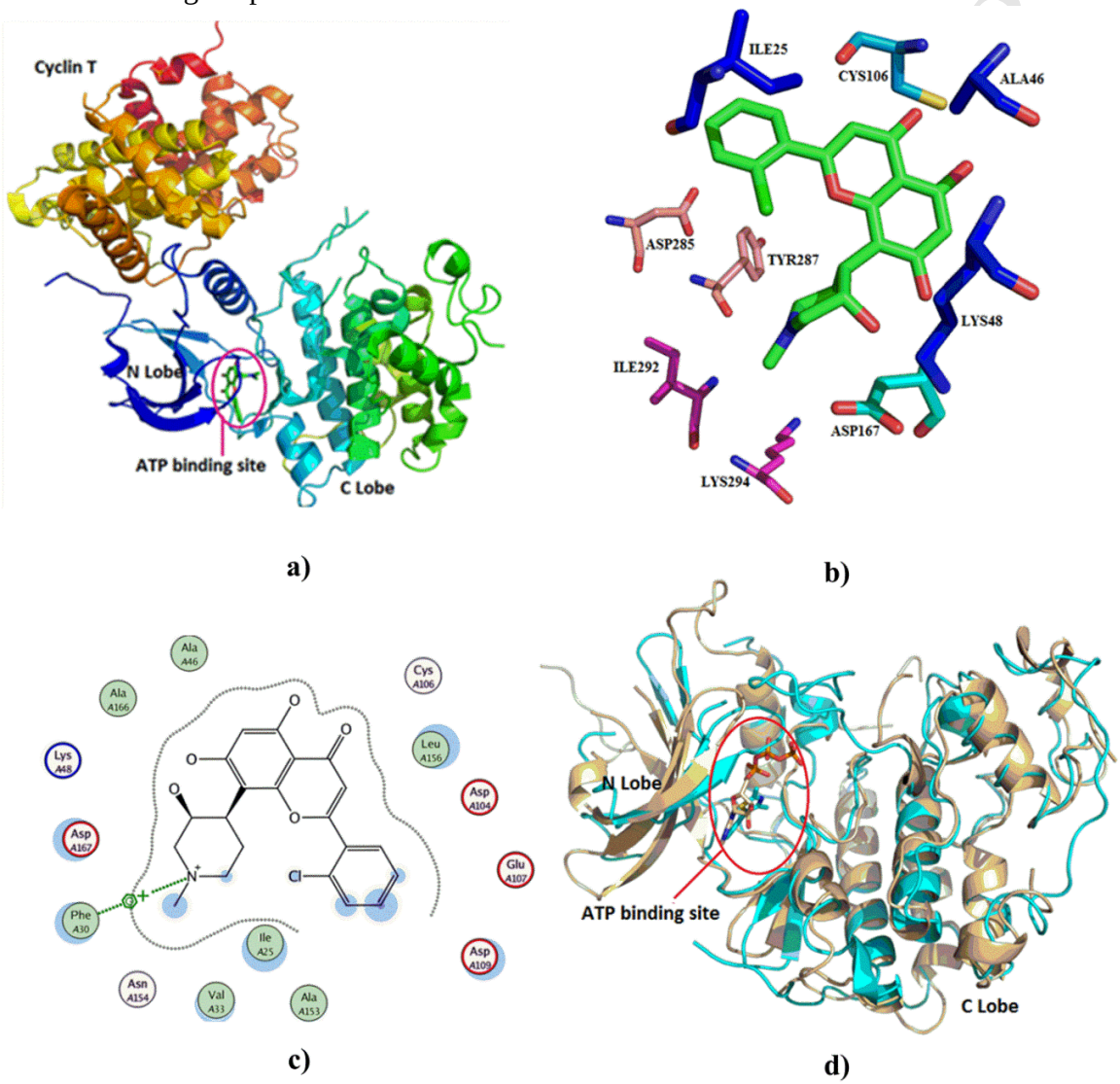

Figure 12. (a) 3D X-ray crystal structure of CDK9 (PDB ID: 3BLR) (b) 3D interaction diagram of bound inhibitor CPB in CDK9 active site (c) 2D interaction diagram depicting critical amino acid residues for the inhibition of CDK9 (d) Aligned proteins showing the identical structures between the chains of CDK9 (wheat color) (PDB ID: 3BLR) and CDK2(cyan color) (PDB ID: 4FKL)

2.9.CDK12

CDK12 gene is located on chromosome 17q12 with a thick band of around 69.2 kbp ranges from 37,618,324 to 37,687,569 on the chromosome. Four crystal structures of CDK12 are known out of which 3 PDBs contains ligands/inhibitors. The available crystal structures include 1170-1238 residues. Generally, CDK12 ligands interact with Mg^{++}, via hydrogen bonds (THR737, LYS756, ASP819, HIS1040, and GLU814) and exhibit hydrophobic interactions (LEU866, and ALA754). The other critical interactions with CDK12 have been given in Table 10 and Figure 13 (b) and (c).

Table 10. X-ray crystal structures available for CDK12

PDB ID	Resolution (Å)	Total residues	Co-crystallized ligand	Ligand interactions with amino acids (if available)	Reference
4CXA	3.15	1198	ANP	THR737, LYS756, ASN864, HIS1040, GLU814, SER863, LEU866	[81]
4NST	2.2	1238	ADP	Mg^{++}, THR737, LYS756, ASP819, HIS1040, GLU814, LEU866, ALA754	[82]
4UN0	3.15	1170	No ligand	----	[81]
5ACB	2.7	1198	5I1	MET816, LEU866, HIS818, GLN1037, CYS1039, ILE733, VAL741	[81]

CDK12 and CDK2 showed sequence similarity of 77.03% and were having 51.35% identical residues (Chart 8 and Figure 13(d)).

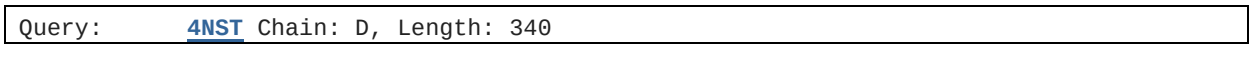

```
Subject:    4FKL Chain: A, Length: 74
Identities: 38/93, i.e., 11.18 % (query) and 51.35 % (subject)
Similars:   57/93, i.e., 16.76 % (query) and 77.03 % (subject)

    4NST.D 12 VDKFDIIGIIGEGTYGQVYKAKDKDTGELVALKKVRLDNEKEGFPITAIREIKILRQLIH 71
              .. |  .  ||||||| ||||..| |||.|||||.         | |||||| .|..| |
PDP:4FKLAa  1 MENFQKVEKIGEGTYGVVYKARNKLTGEVVALKKI--------VPSTAIREISLLKELNH 52

    4NST.D 72 RSVVNMKEIV-TDKQDALDFKKDKGAFYLVFEY103
               ..| . ... |. .            |||||.
PDP:4FKLAa 53 PNIVKLLDVIHTENK----------LYLVFEF 74
Legend: Green - identical residues | Pink - similar residues | Blue - sequence mismatch | Brown - insertion/deletion |
```

Chart 8. Smith Waterman sequence alignment depicting the sequence similarity and difference between the aligned protein CDK12 and CDK2

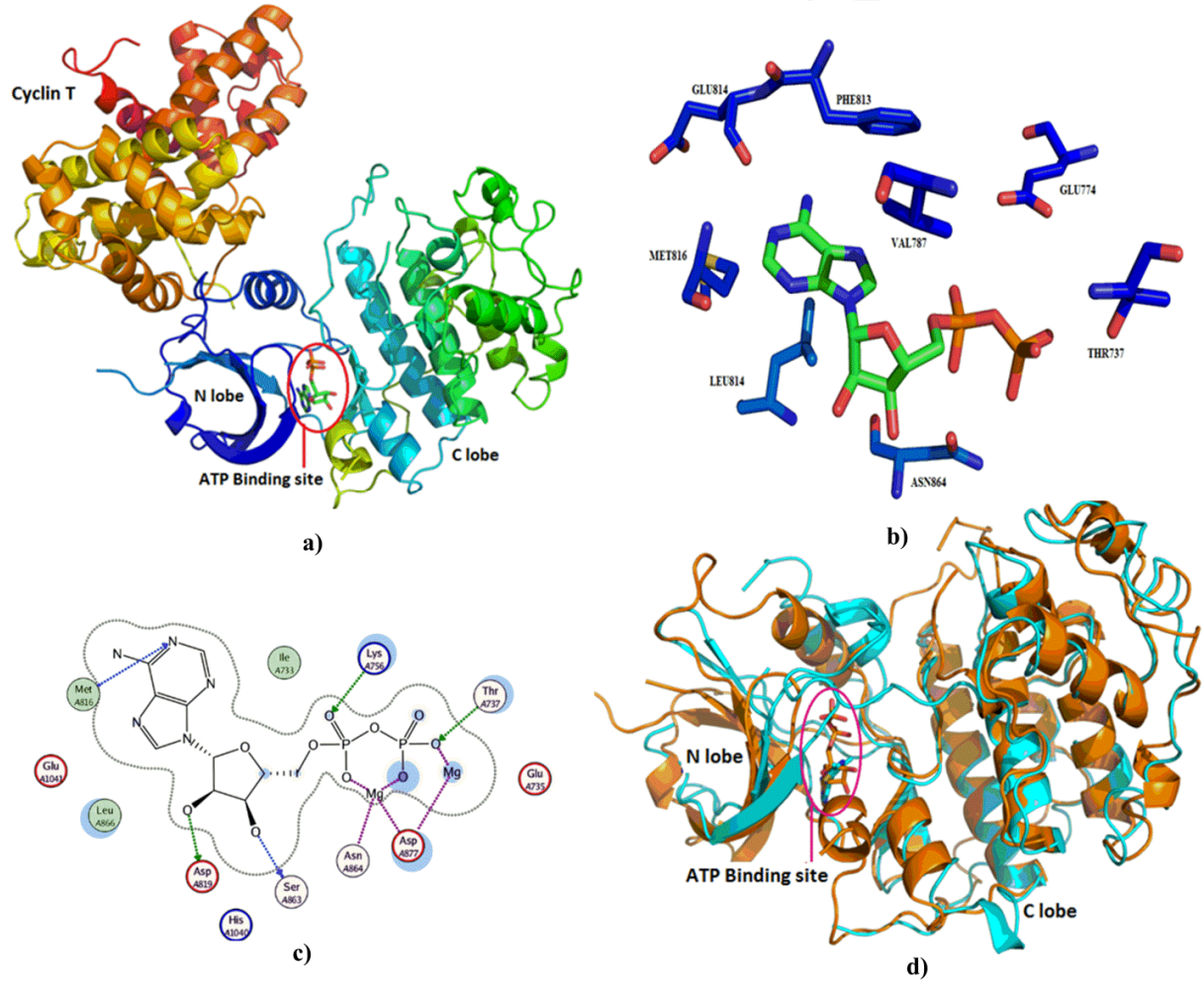

Figure 13. Structural features of Cyclin Dependent Kinase 12 (CDK12) (a) 3D X-ray crystal structure of protein PDB ID: 4NST) (b) 3D interaction diagram of bound inhibitor ADP in

CDK12 active site (c) 2D interaction diagram depicting critical amino acid residues for the inhibition of CDK12 (d) Aligned proteins showing the identical structures between the chains of protein CDK12 (orange color) (PDB ID: 4NST) and CDK2 (cyan color) (PDB ID: 4FKL).

2.10. CDK13

CDK13 is located on chromosome 7p14.1. Only one crystal structure of CDK13 (PDB ID: 5EFQ) (Figure 14a) has been reported so far with a good resolution containing ADP. It contains about 347 residues. Hydrogen bonding interactions with LYS734, THR715, SER841, ASP797, MET794, GLU792, and hydrophobic interactions with LEU844, VAL719 of CDK13 with ADP were found to be important (Table 11, Figure 14 (b) and (c)).

Table 11. X-ray crystal structure of CDK13

PDB ID	Resolution (in Å)	Total residues	Co-crystallized ligand	Ligand interactions with amino acids (if available)	Reference
5EFQ	2.0	347	ADP	LYS734, THR715, SER841, ASP797, MET794, GLU792, LEU844, VAL719	[83]

For the comparison of the structural features, upon sequence alignment of CDK13 with CDK2, 16.43% similar residues and 11.53% identical residues were observed (Chart 9 and Figure 14(d)).

```
Query:      5EFQ chain: C, Length: 347
Subject:    4FKL Chain: A, Length: 74
Identities: 40/92, i.e., 11.53 % (query) and 54.05 % (subject)
Similars:   57/92, i.e., 16.43 % (query) and 77.03 % (subject)

    5EFQ.C 10 VDKFDIIGIIGEGTYGQVYKARDKDTGEMVALKKVRLDNEKEGFPITAIREIKILRQLTH 69
              .. |  .  ||||||| |||||.| |||.|||||.         | |||||| .|..| |
PDP:4FKLAa  1 MENFQKVEKIGEGTYGVVYKARNKLTGEVVALKKI--------VPSTAIREISLLKELNH 52

    5EFQ.C 70 QSIINMKEIVTDKEDALDFKKDKGAFYLVFEY101
               .|. . ...   |. |         |||||.
PDP:4FKLAa 53 PNIVKLLDVI-HTENKL---------YLVFEF 74
Legend: Green - identical residues | Pink - similar residues | Blue - sequence mismatch | Brown - insertion/deletion |
```

Chart 9. Smith Waterman sequence alignment is depicting the sequence similarity and difference between the aligned protein CDK13 and CDK2

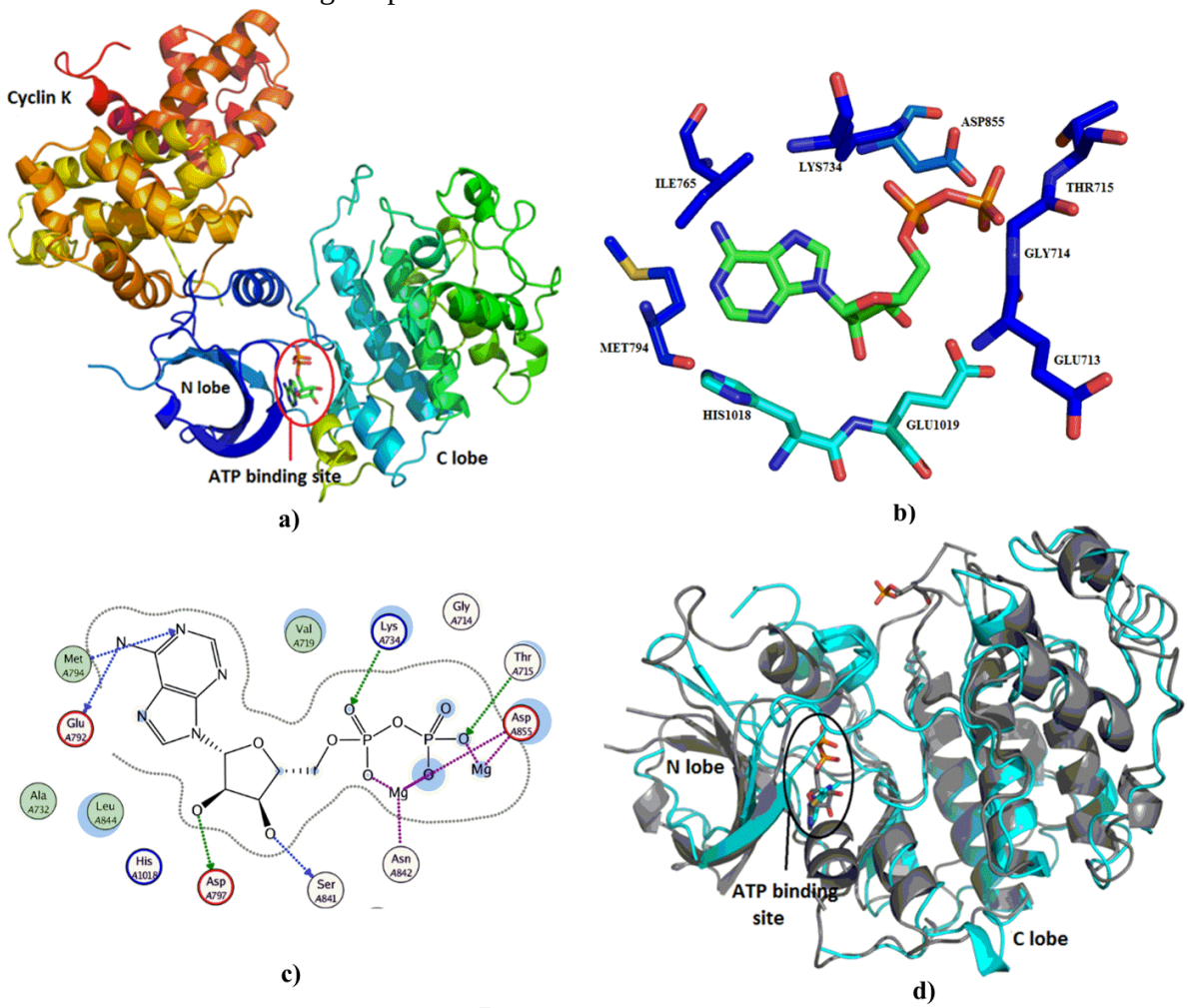

Figure 14. (a) 3D X-ray crystal structure of CDK13 (PDB ID: 5EFQ) (b) 3D interaction diagram of bound inhibitor ADP in CDK13 active site (c) 2D interaction diagram depicting critical amino acid residues for the inhibition of CDK13 (d) Aligned proteins showing the identical structures between the chains of protein CDK13 (gray color) (PDB ID: 5EFQ) and CDK2 (cyan color) (PDB ID: 4FKL)

2.11. CDK16

CDK16 gene is located on chromosome X at the shorter pter (p) arm. It positions 11 with a thin band of around 5.2 kbp ranges from 47,082,956 to 47,088,167 on the chromosome. Only one crystal structure of CDK16 (PDB ID: 3MTL) is available with the indirubicin (Figure 15a) which occupies the CDK16 active site by forming hydrogen bonding interactions with ALA303,

VAL179, LEU 171 and hydrophobic interactions with GLU241, LEU243 (Table 12 and Figure 15 (b) and (c)).

Table 12. X-ray crystal structure of CDK16

PDB ID	Resolution (in Å)	Total residues	Co-crystallized ligand	Ligand interactions with amino acids (if available)	Reference
3MTL	2.4	324	Indirubicin	GLU241, LEU243, ALA303, VAL179, LEU 171	[84]

There was huge similarity (78.38%) between CDK16 and CDK2 active site residues (Chart 10 and figure 15(d)).

```
Query:      3MTL chain: A, Length: 324
Subject:    4FKL chain: , Length: 74
Identities: 46/81, i.e., 14.20 % (query) and 62.16 % (subject)
Similars:   58/81, i.e., 17.90 % (query) and 78.38 % (subject)

    3MTL.A  1 METYIKLDKLGEGTYATVYKGKSKLTDNLVALKEIRLEHEEGAPCTAIREVSLLKDLKHA 60
              || . |..|.|||||  ||| ..|||  .||||.|        | |||||.||||.| |
PDP:4FKLAa  1 MENFQKVEKIGEGTYGVVYKARNKLTGEVVALKKI-------VPSTAIREISLLKELNHP 53

    3MTL.A 61 NIVTLHDIIHTEKSLTLVFEY 81
              ||| | |.||||  | ||||.
PDP:4FKLAa 54 NIVKLLDVIHTENKLYLVFEF 74
```

Legend: *Green - identical residues | Pink - similar residues | Blue - sequence mismatch | Brown - insertion/deletion |*

Chart 10. Smith Waterman sequence alignment depicting the sequence similarity and difference between the aligned protein CDK16 and CDK2

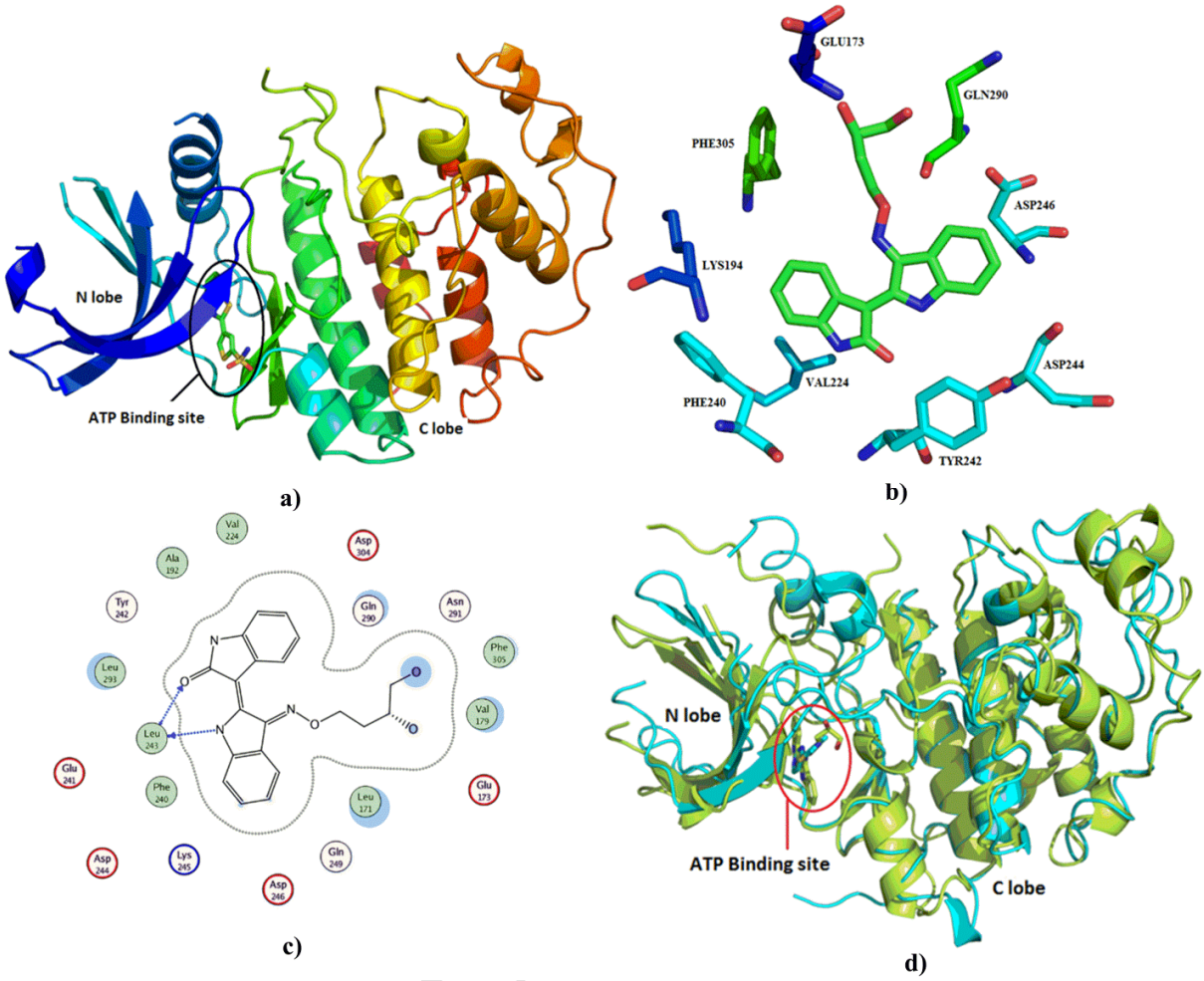

Figure 15. (a) 3D X-ray crystal structure of CDK16 (PDB ID: 3MTL) (b) 3D interaction diagram of bound inhibitor indirubicin in CDK16 active site (c) 2D interaction diagram depicting important amino acid residues for the inhibition of CDK16 (d) Aligned proteins showing the identical structures between the chains of protein CDK16 (lemon color) (PDB ID: 3MTL) and CDK2 (cyan color) (PDB ID: 4FKL)

3. Specificity of the CDKs: The structural insights leading to design of specific inhibitors

The criteria affecting the ligand-receptor interaction and specificity are:-

3.1.Active site residues of the CDKs

3.2.Ligand – CDK binding

3.3.Structural features of ligand

3.1. Active site residues of the CDKs

For the sake of discussion on the uniqueness of CDKs, we considered three broad factors involving differences in active site residues at same positions, the presence of additional residues and conformational changes in the active site residues among ATP sites of various CDKs contributing to the specificity.

3.1.1. Differences between the critical active site residues of the CDKs

The substitution of the smaller active site residues SER84 and MET85 in the CDK1 with the more polar and bulkier HIS84 and GLN85 in CDK2, altered the specificity towards particular inhibitor in such a way that LZ9 could bind with the CDK1 participating in hydrophobic interaction with non-polar MET85; whereas dinacicilib could bind with CDK2 (Figure 16). Dinaciclib is inhibitor of both CDK1 (IC_{50}=3nM) and CDK2 (IC_{50} = 1nM).

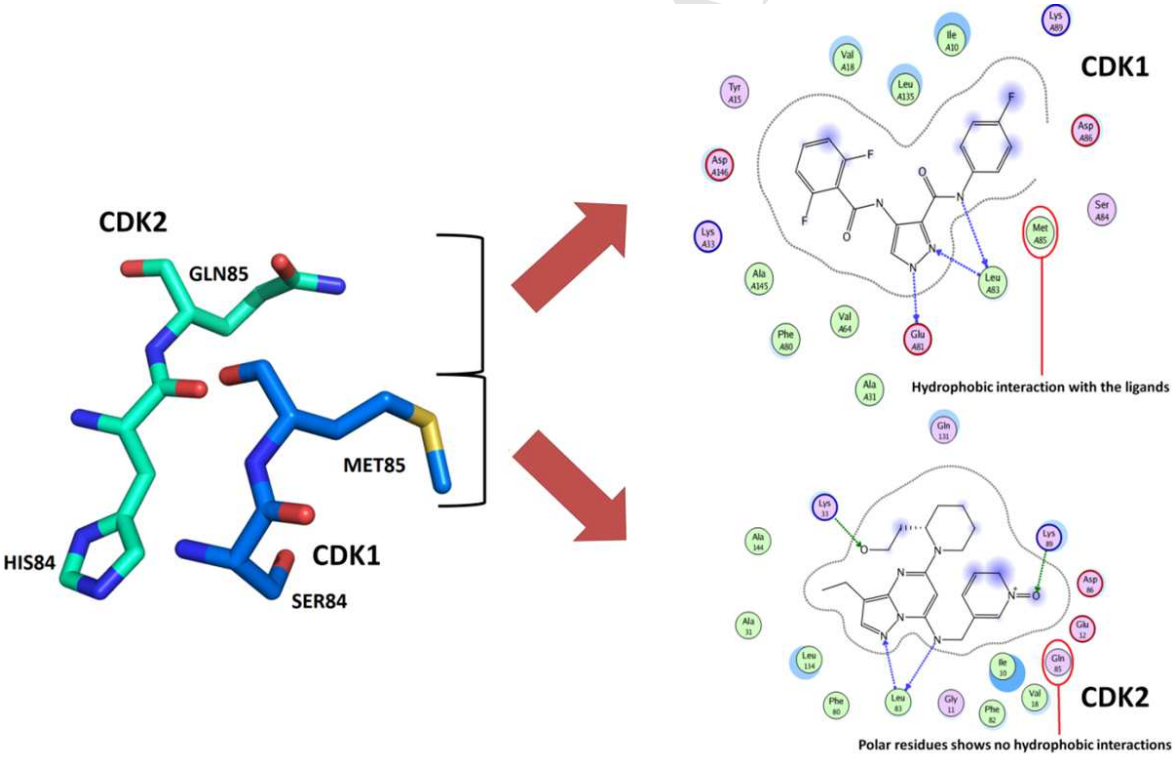

Figure 16. Illustrative representation of CDK1 and CDK2 active site residues differences that may alter the specificity of ligand binding

3.1.2. Additional residues and their nature present in CDKs active site

The presence of the other residues and their environment in the active site of the CDKs may alter the specificity of ligand binding to the active site of the protein. It can be explained in context with CDK1 and CDK2. In CDK1, TYR15 is present in the active site and is absent in the CDK2. In CDK2, GLY13 is present as an additional residue in the active site. TYR15 is polar in nature while GLY13 is nonpolar. The nature of amino acid present in active site changes the polarity of a region, restricting the binding of a ligand to that part and hence alters the specificity. Figure 17 represents the additional residues that affect the binding affinity and specificity of the ligand to that part of CDKs.

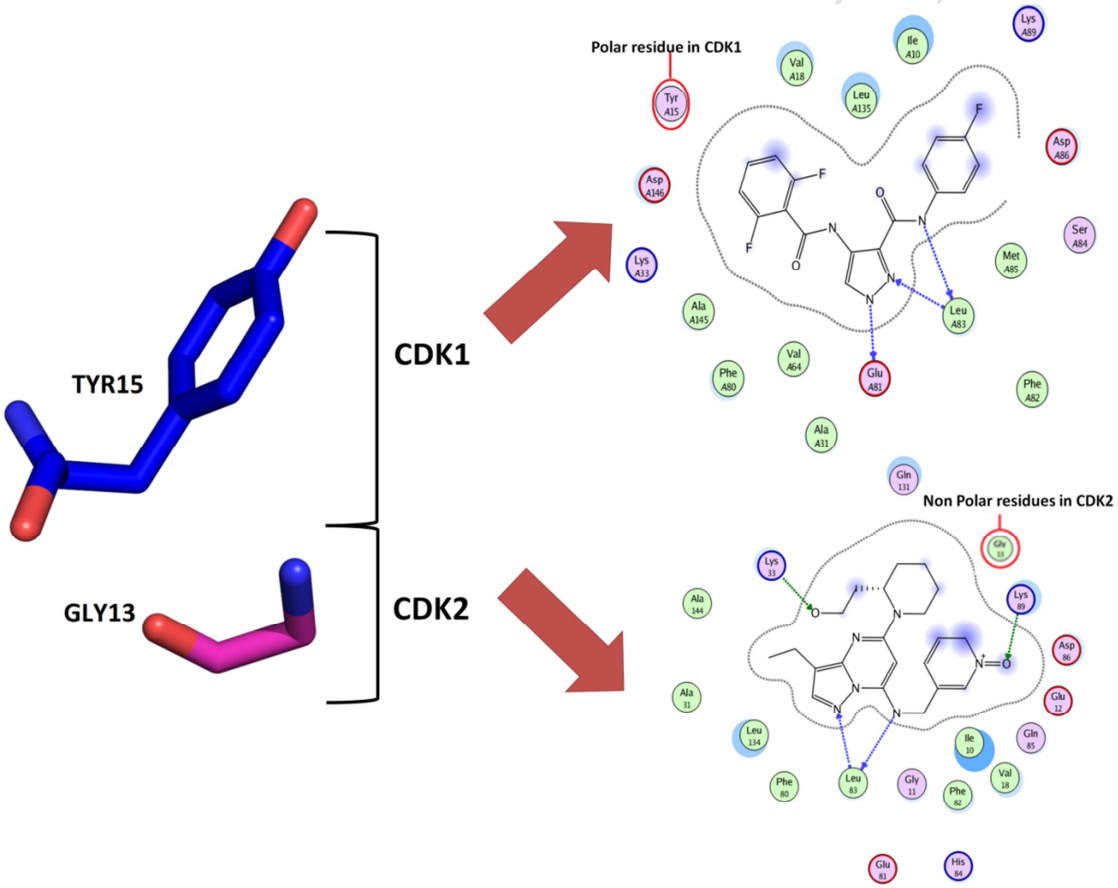

Figure 17. Illustrative representation of CDK1 and CDK2 active site residues where the presence and nature of the additional residues alter the specificity of ligand binding

Thus factors that affect the specificity of dinacicilib are results of amino acid interactions and their nature (Figure 17).

3.1.3. Different conformational modes of the similar residues in the active site of the CDKs

The various conformational modes of residues affect the ligand-CDK interactions to a greater extent and also involve all types of interactions namely hydrogen bonding, van der Waal, hydrophobic and stacking interactions. The conformational change in the residues may also affect the atomic distance between the ligand functional groups and hence decrease or increase the specificity.

The conformational differences are explained in context to the CDK1 and CDK2 active sites. It was observed that for the same residues in the active site, there was a different conformation of the residues which may be on account to the folding of the proteins. The folding patterns of both CDK1 and CDK2 are different. The main impact of this folding is seen on LYS residues. The LYS33 and LYS89 residues show a different pattern of the arrangement in the active site of both the CDKs. The significant illustration is depicted in Figure 18.

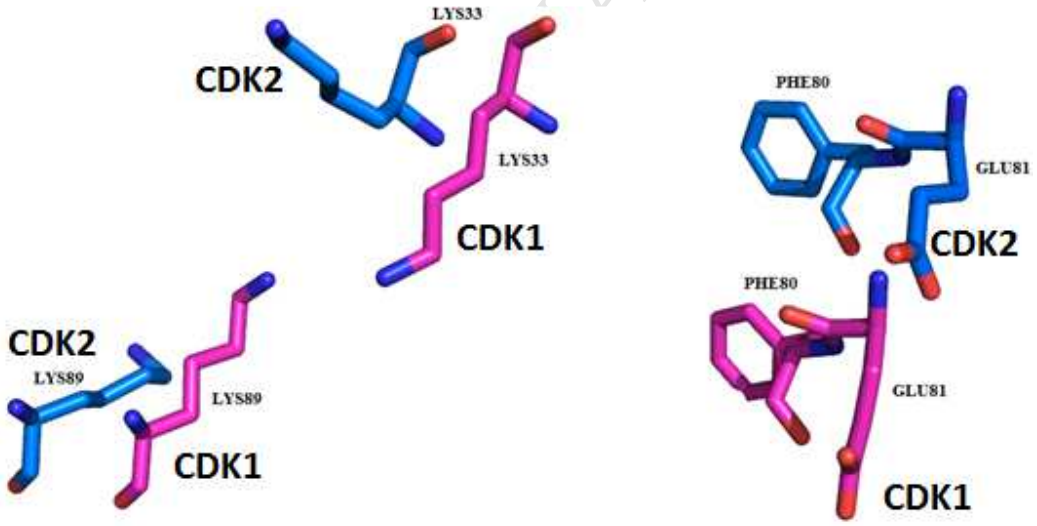

Figure 18. 3D representation of the conformational differences between CDK1 (Pink) and CDK2 active site residues (Blue)

The comparison between the active site residues has been made for most of the CDKs highlighting the distinct differences (Table 13). It can be perceived that LYS residue is conserved in all the CDKs (Table 13); LYS33 (CDK1, CDK2, and CDK5), LYS43 (CDK6), LYS41 (CDK7 and CDK8), LYS48 (CDK9), LYS756 (CDK12), LYS194 (CDK13) and

LYS734 (CDK16). CDKs have one or more important active site amino acid residues that are mainly responsible for the Ligand-CDK interactions affecting the specificity. For example LEU83 (CDK1 and CDK2), CYS83 (CDK5), CYS106 (CDK9), VAL101 (CDK6), MET94, MET 816, MET794 (CDK7, CDK12, and CDK16, respectively), ALA100 (CDK8) and LEU243 (CDK13) were found to be critical for the activity as well as specificity as they differ in the nature and hence affect the specific nature in the ligand-CDKs interactions. The spatial arrangement of the all the residues have been depicted Figure S1 (in supplementary data).

ACCEPTED MANUSCRIPT

Table 13: Active site residues of some CDKs (with the available PDB IDs) which contribute towards the specificity of inhibitors

CDK1	CDK2	CDK4	CDK5	CDK6	CDK7	CDK8	CDK9	CDK12	CDK13	CDK16
ILE10	ILE10	ILE12	ILE10	ILE19	LEU18	VAL27	ILE25	ILE733	ILE711	LEU171
GLY11	GLY11	GLY13	GLY11	GLY20	GLY19	GLY28	GLY26	GLY734	GLY712	GLY172
GLU12	GLU12	VAL14	GLU12	GLU21	GLU20	ARG29	GLN27	GLU735	GLU713	GLU173
GLY13	GLY13	GLY15	GLY13	GLY22	GLY21	GLY30	GLY28	GLY736	GLY714	GLY174
THR14	THR14	--------	THR14	---------	GLN22	THR31	THR29	THR737	THR715	---------
TYR15	TYR15	ALA16	TYR15	ALA23	PHE23	TYR32	---------	TYR738	---------	---------
GLY16	GLY16	GLY18	GLY16	GLY25	ALA24	---------	---------	---------	---------	ALA177
VAL18	VAL18	VAL20	VAL18	VAL27	VAL26	VAL35	---------	VAL741	VAL719	VAL179
ALA31	ALA31	ALA33	ALA31	ALA41	ALA39	ALA50	ALA46	ALA754	---------	ALA192
LYS33	LYS33	LYS34	LYS33	LYS42	LYS41	LYS41	LYS48	LYS756	LYS734	LYS194
GLU51	ILE52	---------	GLU51	---------	---------	GLU60	---------	GLU774	---------	GLU211
---------	---------	---------	---------	---------	---------	---------	---------	---------	---------	VAL212
LEU55	LEU55	---------	LEU55	---------	---------	---------	LEU70	LEU778	---------	---------
LEU58	---------	---------	---------	---------	---------	---------	---------	LEU781	---------	LEU218
VAL64	VAL64	VAL71	VAL64	VAL76	---------	---------	VAL79	VAL787	---------	VAL224
PHE80	PHE80	---------	PHE80	---------	PHE91	PHE97	PHE103	PHE813	PHE791	PHE240
GLU81	GLU81	GLU94	GLU81	---------	---------	ASP98	ASP104	GLU814	GLU792	GLU241
PHE82	PHE82	HIS95	PHE82	HIS100	PHE93	TYR99	PHE105	TYR815	TYR793	TYR242
LEU83	LEU83	VAL96	CYS83	VAL101	MET94	ALA100	CYS106	MET816	MET794	LEU243
SER84	HIS84	ASP97	ASP84	ASP102	GLU95	GLU101	GLU107	ASP817	---------	ASP244
MET85	GLN85	GLN98	GLN85	GLN103	THR96	---------	---------	HIS818	---------	LYS245
ASP86	ASP86	ASP99	ASP86	ASP104	ASP97	ASP103	ASP109	ASP819	ASP797	ASP246
LYS89	LYS89	THR102	LYS89	THR107	---------	HIS106	---------	GLY822	HIS1018	GLN249
HIS126	---------	----------	---------	---------	---------	---------	---------	HIS857	GLU1019	---------
---------	---------	----------	---------	---------	---------	---------	---------	---------	---------	VAL282
LYS130	LYS129	LYS141	LYS128	LYS146	LYS139	LYS153	LYS151	LYS861	---------	LYS288
GLN132	GLN131	GLU144	GLN130	GLN149	GLN141	ALA155	ALA153	SER863	SER841	GLN290
ASN133	ASN132	ASN145	ASN131	ASN150	ASN142	ASN156	ASN154	ASN864	ASN842	ASN291
LEU135	LEU134	LEU147	LEU133	LEU152	LEU144	LEU158	LEU156	LEU875	LEU844	LEU302
ALA145	ALA144	ALA157	ALA143	ALA162	ALA154	ALA172	ALA166	ALA876	ALA854	ALA303
ASP146	ASP145	ASP158	ASP144	ASP163	ASP155	ASP173	ASP167	ASP877	ASP855	ASP304
PHE147	PHE146	PHE159	PHE145	PHE164	PHE156	MET174	PHE168	PHE878	---------	PHE305
GLY148	GLY147	GLY160	GLY146	GLY165	GLY157	GLY175	GLY169	GLY879	---------	GLY306
---------	LEU148	----------	---------	---------	LEU158	PHE176	---------	---------	GLU752	LEU307
GLY153	GLY153	----------	---------	---------	---------	---------	---------	---------	---------	---------
VAL154	VAL154	----------	---------	---------	---------	---------	---------	---------	---------	---------

3.2. Ligand-CDK binding

The binding energy of the ligand-CDK complex and ligand-CDK interactions are other factors that could affect the specificity.

3.2.1. Binding energy of ligand-CDK complex

The binding energy of the ligand-CDK complex reflects the structure specificity of ligand that binds to the CDK [85]. We performed the binding affinity studies including 10 CDKs and their co-crystal ligands [86]. The binding energy was calculated (equation 1) by calculating the potential energy of CDK, the potential energy of ligand, and potential energy of ligand-CDK complex.

$$\Delta G(Binding\ free\ energy) = G(Potential\ energy\ of\ complex) - G(Potential\ energy\ of\ CDK) - G(Potential\ energy\ of\ ligand) \ldots\ldots\ldots \text{ Equation 1}$$

The potential energy of ligands bound to the CDKs and CDK protein was calculated using the prime [87]. The binding energies are shown in Table 14 with their respective CDKs and potential energies of the ligand, CDK and ligand-CDK complex.

The binding energy of the CDK7 with ATP was observed to be -62.626 Kcal/mol, which elucidates strong binding of the ATP with CDK7 protein. Thus for the development of CDK7 competitive inhibitor at the ATP binding site, the binding affinity of the ligand/inhibitor has to be equal to or more than ATP. In the same way, the binding energy of CDK8 with OSR is predicted to be -58.07 Kcal/mol. It shows that OSR is a good competitive inhibitor of ATP and binds strongly to CDK8.

Table 14: Binding energies of the ligands bound to specific CDKs

CDK	PDB ID	Ligand	P.E.(LR)	P.E.(R)	P.E.(L)	ΔG(Binding energy)

CDK1	4Y72	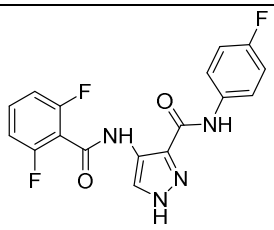 LZ9	7097.051	7066.381	72.966	-42.296
CDK2	4FKL	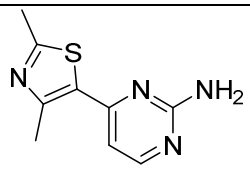 CK2	3182.810	3224.416	-9.537	-32.069
CDK5	1UNH	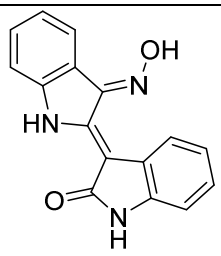 IXM(Indirubicin)	5850.033	5740.317	142.480	-32.764
CDK6	2EUF	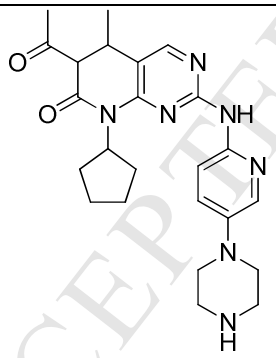 LQQ (Palbocicilib)	8403.919	8220.193	186.014	-2.288
CDK7	1UA2	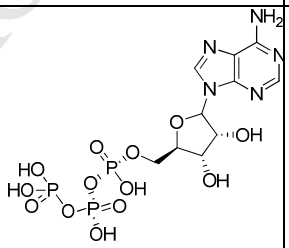 ATP	8389.317	8314.937	137.006	-62.626

ACCEPTED MANUSCRIPT

CDK8	4F6U	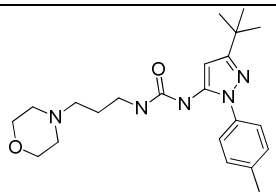 OSR	5210.750	5145.919	122.901	-58.07
CDK9	3BLR	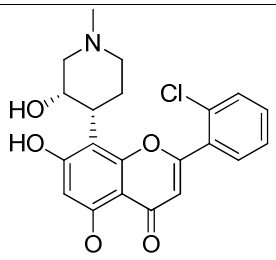 CPB	6372.908	6265.315	147.570	-39.977
CDK12	4NST	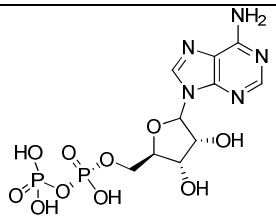 ADP	9414.212	9323.699	117.697	-27.184
CDK13	5EFQ	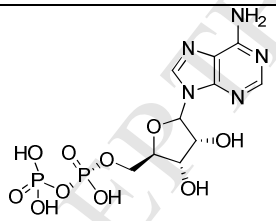 ADP	6505.114	6405.970	107.774	-8.63
CDK16	3MTL	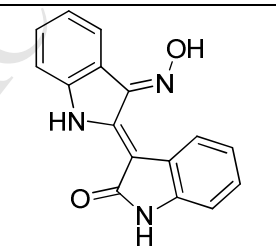 IXM(Indirubicin)	3544.068	3450.116	141.922	-47.97

ACCEPTED MANUSCRIPT

In order to understand the impact of binding energy on ligand-CDK interactions, dinacicilib was docked into CDK1, CDK2, CDK5 and CDK9 and their binding energies were calculated (Table 15). Overall, the reported IC_{50} values and the binding energies were found to be in correlation. Though IC_{50} values of dinacicilib against CDK2 and 5 are same their binding energies are different that could be due to the difference in affinity of dinaciclib towards CDK2 and 5.

Table 15: Representation of the binding energies of dinacicilib with the CDK1, 2, 5 and 9

CDK	**PDB ID**	**P.E.(LR)**	**P.E.(R)**	**P.E.(L)**	**ΔG(Binding energy)**	**IC_{50} (nM)**[88]
CDK1	4Y72	7548.48	7272.21	241.67	-34.6	3
CDK2	4KD1	3949.49	3848.72	153.53	-52.76	1
CDK5	1UNH	6185.08	5878.45	223.34	-83.29	1
CDK9	3BLR	6655.52	6367.36	239.38	-48.78	4

3.2.2. Ligand-CDK interactions

Ligand-protein interactions are the important set of parameters responsible for the specific characteristics of the drugs. The comprehensive sets of parameters are collectively termed as the score. There are different types of score existing that are named according to the software in which those are incorporated. Some of the enlisted terms are a gold score, glide score, chem score, flex score, etc. In the case of CDKs, the interactions were observed through the glide score in MAESTRO 11.1. The specific interactions such as hydrogen bonding, hydrophobic interactions, van der Waal's, etc. comprise a glide score.

To see the effect of ligand-CDK interaction on the specificity the CDK1 inhibitor, LZ9 was docked into all the available CDKs. The pattern of dock score of CDK1 inhibitor (LZ9) in other CDKs is enlisted in Table 16. From the pattern, we can draw the conclusion that the CDK1 inhibitor is specific to CDK1 and not to the other CDKs. The 2D interaction diagrams of LZ9 with CDK2, CDK5, CDK6, and CDK9 have been depicted in Figure 19.

Table 16: Representation of the docking scores of CDK1 inhibitor (LZ9) bound to the different CDKs

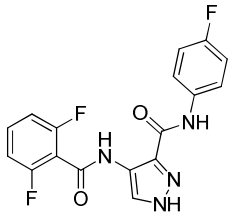

S.no.	CDK	PDB ID	Docking score (bound ligand)	Docking score (CDK1 inhibitor)
1.	CDK1	4Y72	-11.47	-11.47
2.	CDK2	4FKL	-10.67	-6.48
3.	CDK5	1UNH	-7.46	-7.58
4.	CDK6	2EUF	-8.08	-7.06
5.	CDK7	1UA2	-9.78	-6.73
6.	CDK8	4F6U	-12.46	-6.56
7.	CDK9	3BLR	-9.21	-6.02
8.	CDK12	4NST	-12.04	-6.23
9.	CDK13	5EFQ	-11.76	-6.38
10.	CDK16	3MTL	-10.37	-6.87

ACCEPTED MANUSCRIPT

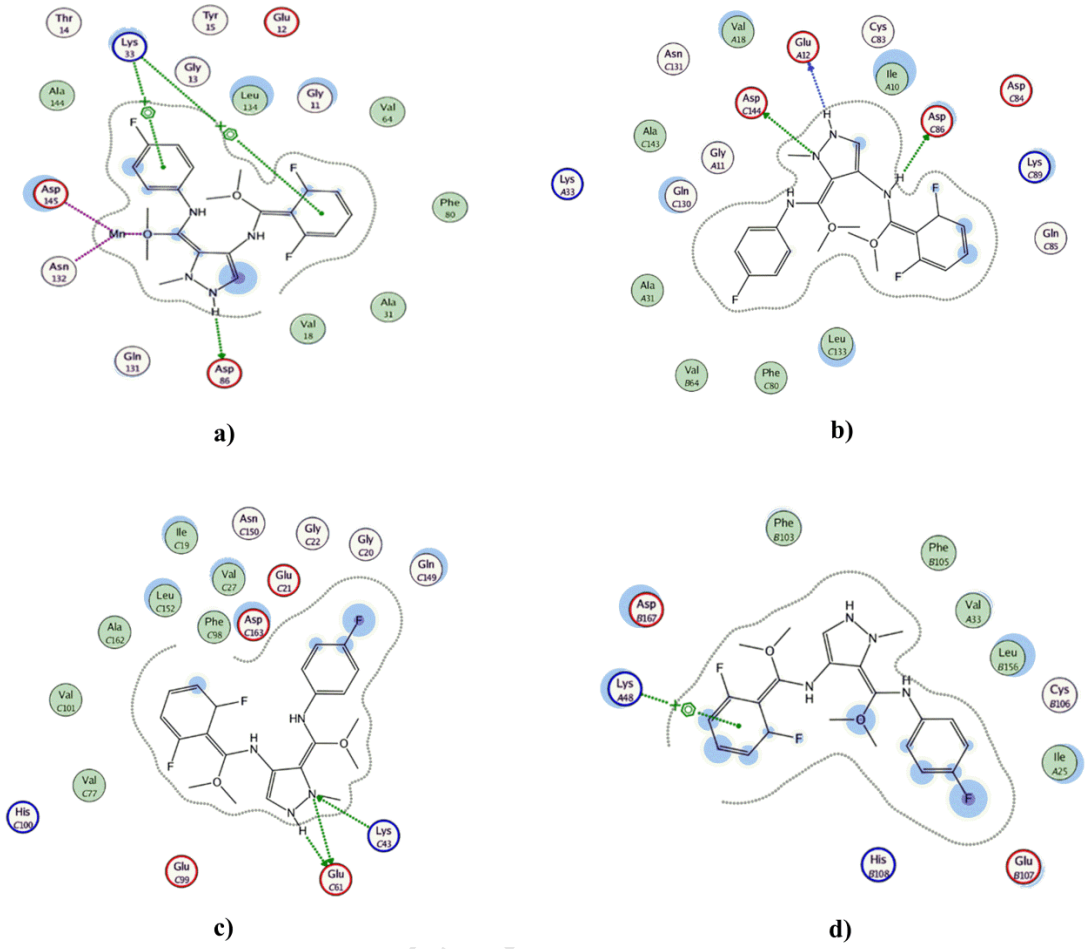

Figure 19. The representation of 2D interaction diagram of CDK1 inhibitor (LZ9) in the active site of CDK2, CDK5, CDK6, and CDK9.

The structure-activity relationship studies explained in a review by Li et al., 2016 highlighted some key structural features that must be taken into consideration for the development of CDKs inhibitors specifically for CDK1, 2, 4, 6 and 9. For a CDK2 inhibitor, hydrogen bonding interactions with GLU81 and LEU83 are the required for the inhibitory potency; the presence of hydrophobic pocket consisting of PHE80, VAL64, HIS84, GLN85 favors the hydrophobic interactions and π-π stacking interactions; ASP145 of the DFG motif and ASP86 of the solvent-exposed region support the ionic interactions. For selective inhibition of CDK1/2, there is a requirement of electrostatics interaction with LYS89, while for selective inhibition of CDK4/6 there is a need of polar interaction with THR99/107. The rare conserved hinge residue hydrogen bonding interaction of HIS92 and VAL101 was also considered necessary for selective CDK4

and CDK6 inhibitors, respectively. Strong hydrogen bonding interactions with ASP167, CYS106 are a necessity for the development of CDK9 inhibitors. In order to understand and correlate the impact of positive and negative interactions with the observed activity, we performed docking studies of alvocidib which is a pan-inhibitor of CDK9 (IC_{50} = 20 nM), CDK1 (IC_{50} = 30 nM) and CDK2 (IC_{50} = 170 nM). It was found to occupy CDK9 active site via electrostatic interactions with ASP167, hydrogen bonding with CYS106 and ASP104. In a similar manner, alvocidib was found to bind with CDK1 (IC_{50} = 30 nM) by interacting with LEU83, GLU81, and GLN132 (hydrogen bonding interactions). It was interesting to note that alvocidib only showed hydrogen bonding interaction with LEU83 but not with GLU81. In addition, it did not exhibit electrostatic interactions with LYS89 and ASP145. This overall supported for the less inhibitory activity of alvocidib against CDK2 (Figure 20).

ACCEPTED MANUSCRIPT

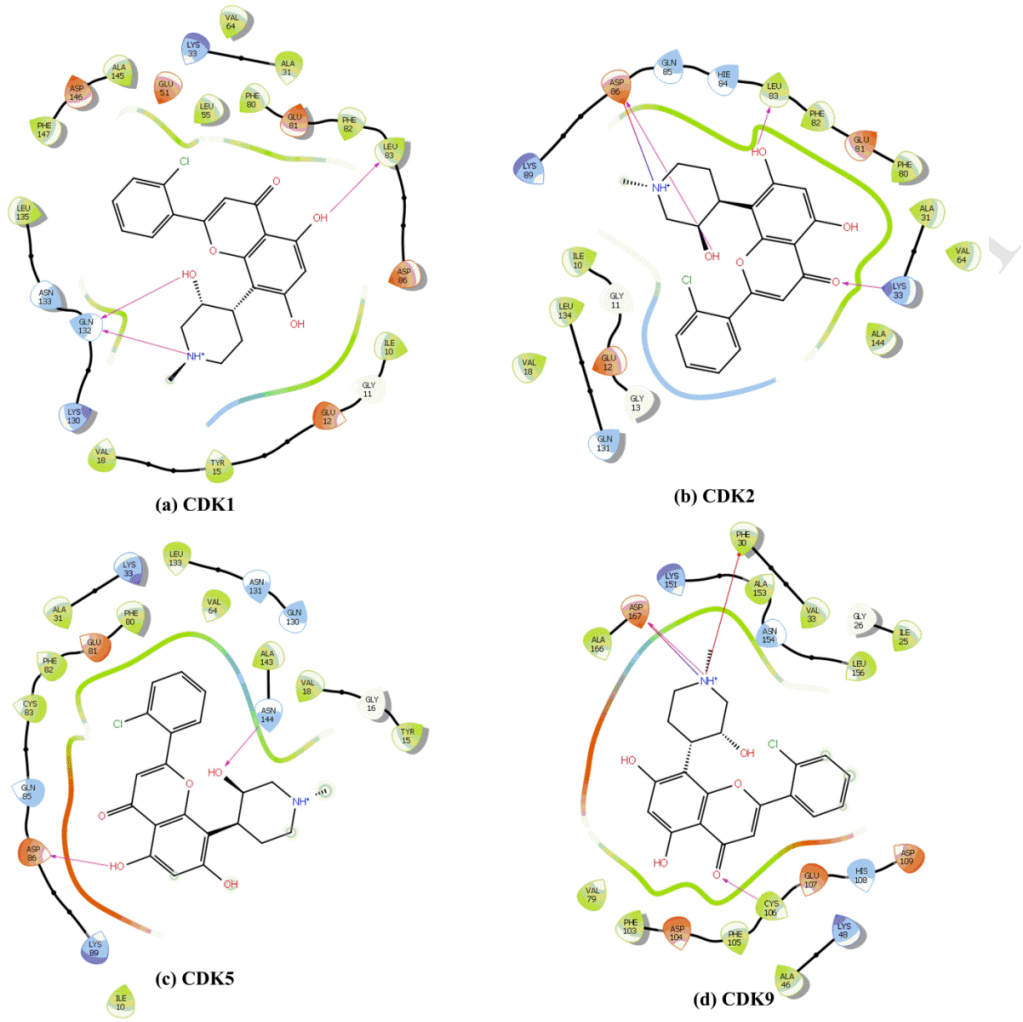

Figure 20: 2-D interaction diagram of alvocidib which is pan inhibitor of CDK9 (20 nM), CDK1 (30 nM) and CDK2 (170 nM).

Further, the role of cysteines has been found responsible for the covalent binding of the inhibitors that are accommodated in the ATP binding site [89, 90]. Recently, remote cysteines have been exploited for the design of covalent inhibitors present in the CDK7 (THZ1), CDK12 (THZ531) and CDK13 (THZ531) at 16.5Å, 11.7Å, and 11.7Å, respectively (Figure 21) [91]. In order to find out the accessibility of cysteine residues near the active site, we aligned all the available crystal structures of CDK1, CDK2, CDK4, CDK5, CDK6, CDK7, CDK8, CDK9, CDK12, CDK13 and CDK16 (See supplementary content; Figure S1). It was observed there are CYS83 in CDK5 and CYS106 in CDK9 present in the active site and are essential for the interaction with ligands. The availability of CYS118 at 16.8Å in CDK1, CYS119 at 15.4.8Å in

CDK2, CYS15 at 13.6Å in CDK6 and CYS84 at 9.9Å in CDK8 hold scope for covalent inhibitor design (See supplementary content; Figure S3 and Table S5).

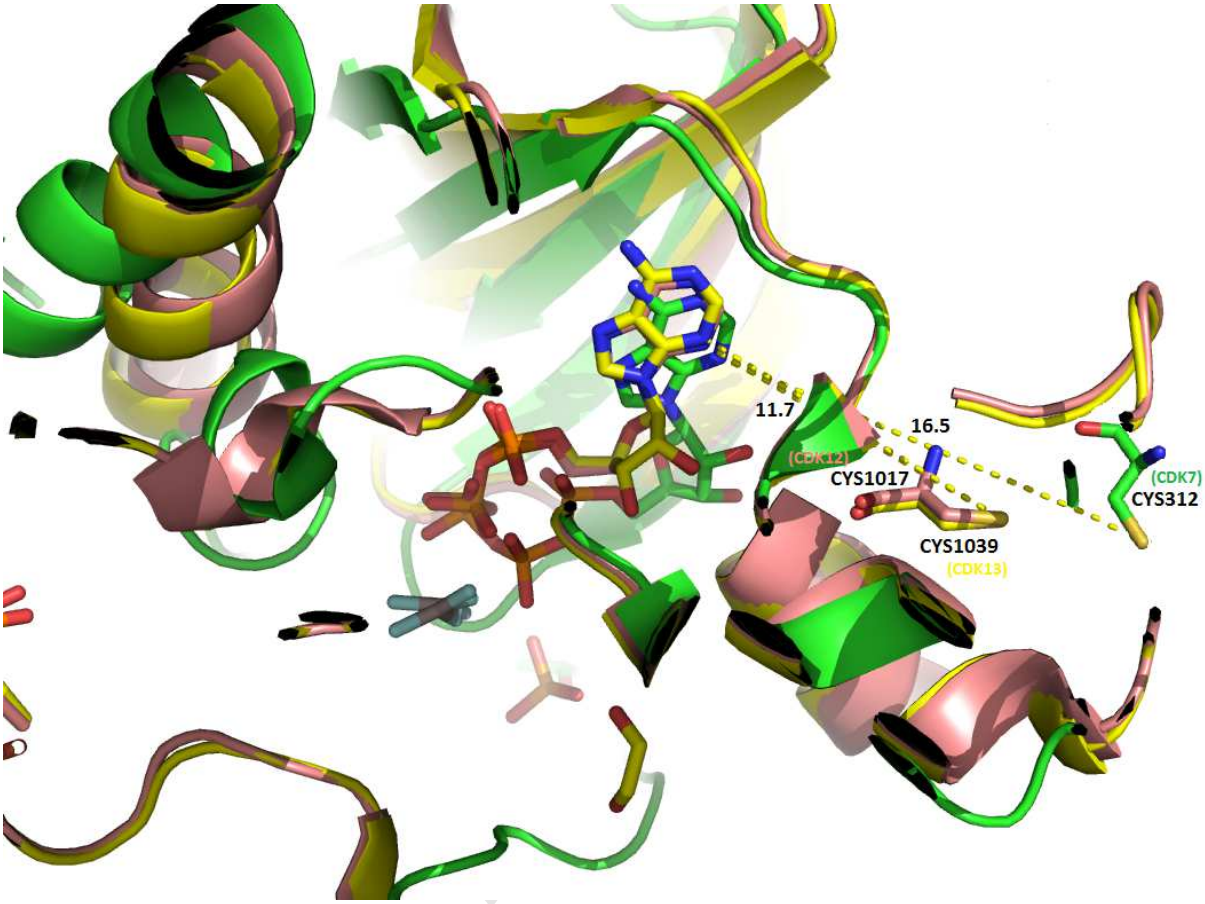

Figure 21. Remote cysteines present in CDK7 (green), CDK12 (Peach) and CDK13(yellow) and are targeted for the covalent binding of the inhibitors.

Palbocicilib and ribocicilib are both inhibitors of CDK4 and 6. As the X-ray structure of CDK4 was not available with either ligand or inhibitor, we aligned active site residues of CDK4 (PDB ID: 2W9Z) and CDK6 (PDB ID: 2EUF) in order to explain non-specificity of the drugs towards CDK4 and 6. There was only one amino acid difference (GLU144 in CDK6 and GLN149 in CDK4) in the active site of both the proteins (Figure 22 and Supplementary content table S6) [92, 93].

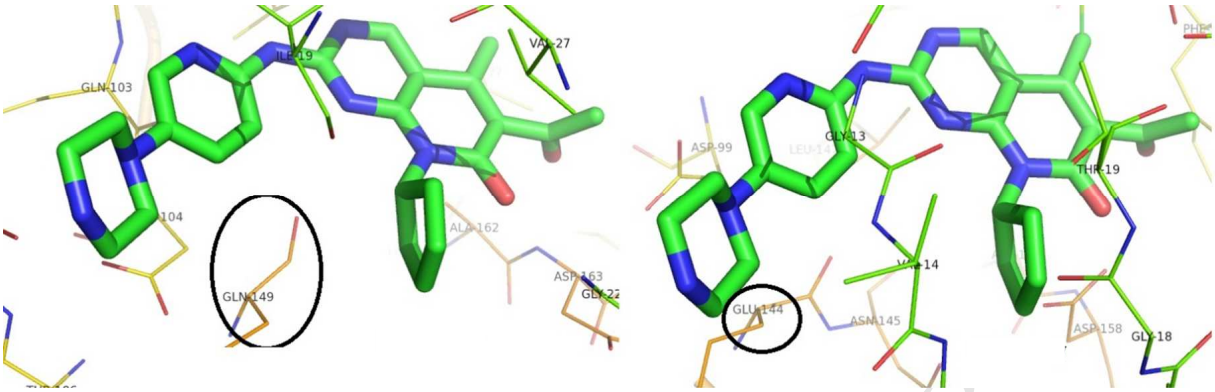

Figure 22. The cmparison between the active site of CDK6 (PDB ID: 2EUF) and CDK4 (PDB ID: 2W9Z).

3.3. Structural features of ligand

Other than the structural similarity features and ligand-receptor interactions, structural features of ligands also contribute to the specificity to the particular CDKs. The structural features include the Constitutional descriptors, Ring descriptors, Topological indices, Walk and path counts, Connectivity Indices, 2D matrix-based descriptors, Burden eigen values, 2D autocorrelations, Geometrical descriptors[94], 3D matrix-based descriptors, 3D-MoRSE descriptors[95], 3D autocorrelations, Functional group counts, WHIM descriptors [96], GETAWAY descriptors[97], Atom-centred fragments, Atom-type E-state indices, and Drug-like indices[97]. The inhibitors bound to the different CDKs were calculated for their descriptors using the PADEL descriptor calculator [98, 99]. The table 17 shows the inhibitors bound to different CDKs were correlated to some relevant descriptors.

The design of the particular CDK inhibitor on the basis of descriptors can be explained well by taking the example of CDK4/6 inhibitors. Not much significant differences were observed in the values of the descriptors HOMO, LUMO, Free accessible surface area, the diameter of a molecule, Vander Waal's volume, etc. The differences between the values of the descriptors can be treated as the range that can help design the better molecules with increased specificity towards the particular CDK. The comparison between the descriptors of three CDK4/6 inhibitors namely palbociclib, abemaciclib and ribociclib were done. The range values can be set for the appropriate descriptor, and a new molecule with a better specificity and activity can be designed. The field values of descriptors such as dipole (4-6), HOMO (-8 to -9), LUMO (0 to -1),

Accessible surface area (ASA) (700-800), balbanJ (1-1.5), BCUT (0.5-0.6), Polarity (40-50), density (0.7-0.75), diameter (15-20), Energy (75-85), drug likeliness (1), molecular refractivity (12-15), log P (1-4), van der Waal area (450-500), van der Waal volume (600-700), volume (400-500) exemplified the importance of descriptors in design of inhibitor particularly for CDK4/6. The important descriptor values were calculated and are enlisted for the CDK4/6 inhibitors in Table 17 and 18.

ACCEPTED MANUSCRIPT

Table 17: Descriptor values calculated for the available CDK4/6 inhibitors-Part 1

CDK4/6 inhibitor	dipole	HOMO	LUMO	ASA	balabanJ	BCUT	pol	density	diameter
Abemacicilib	5.79	-8.79	-0.79	847.47	1.09	0.56	49.27	0.74	20
Palbocicilib	4.98	-8.54	-0.86	723.59	1.20	0.56	43.29	0.73	16
Ribocicilib	5.50	-8.91	-0.68	741.84	1.17	0.62	44.97	0.72	16

Table 18: Descriptor values calculated for the available CDK4/6 inhibitors-Part 2

CDK4/6 inhibitor	Energy	Druglike	logP(o/w)	mr	vdw_area	vdw_vol	vol	Weight
Abemacicilib	69.34	0	3.56	13.95	507.95	682.68	487	506.60
Palbocicilib	80.81	1	1.16	12.47	435.87	606.20	430.25	448.55
Ribocicilib	71.50	1	1.62	12.21	441.63	598.49	426.13	434.54

ACCEPTED MANUSCRIPT

The difference in sequences of CDKs and their critical amino acid residues could be exploited for design of a specific CDK inhibitor. The essential amino acid interactions include LEU83, MET85 (CDK1), LEU83, ASP86 (CDK2), CYS83 (CDK5), CYS106 (CDK9), VAL101 (CDK6), MET94, MET 816, MET794 (CDK7, CDK12, and CDK16, respectively), ALA100 (CDK8) and LEU243 (CDK13). There are small differences in CDK1 and CDK2 active site, MET85 in CDK1 is one of the important residues required for hydrogen bond interaction while it is replaced with GLN85 (polar residue) and is not a key residue for the interaction in CDK2. ASP86 is significant amino acid residue in CDK2 active site required for hydrogen bond interaction while it is absent in CDK1. The orientation of LYS residues is different in CDK1 and 2 which are likely to affect the ligand binding to a greater extent. The ligand-CDK complex binding energy is another important parameter which can be taken into account while designing a specific CDK inhibitor. For example, the binding energy of dinacicilib to both CDK1 and CDK2 differs and is -34.6 kcal/mol and -52.76 kcal/mol, respectively which gives the idea that CDK2-dinacicilib complex is more stable than CDK1-dinacicilib complex as conferred from IC_{50} values. The accessible surface area and volume of the ligand also affect the binding of the ligand to CDK subtypes and range dissimilar. In order to design a selective covalent inhibitor of CDKs, the distance between ligand and a remote cysteine residue (X-ray structures) of a particular CDK should be considered. This has been well explained by taking examples (Figure 21) such as THZ1 (CDK7 inhibitor) and THZ531 (CDK12, and CDK13 inhibitor). The remote cysteine residues in case of other CDKs could be targeted for the design of specific CDK inhibitor by taking into account their distances (Table S5, Figure S3) from respective ligands. Thus the above information and discussion could be useful for selective CDK inhibition.

Conclusion

Among all the essential proteins involved in cell division, cyclin-dependent kinases are the most imperative. CDKs comprise of the multifunctional enzymes that can transform various protein substrates associated with the cell cycle progression. CDKs are found to be extensively involved in cancer both directly and through crosstalk(s) cascades including mitogenic and non-mitogenic dependent pathways. Till date, few CDK inhibitors are discovered, but they lack specificity hence commonly abbreviated as Pan Inhibitors. In this league, the revolutionary introduction of CDK 4/6 inhibitor palbociclib has led to the idea of specific inhibitors of CDKs. After the

palbociclib approval, other drugs abemacicilib and ribociclib were introduced, and in the current year these were approved as CDK4/6 inhibitors. However, the design of the specific CDK inhibitor has remained a challenge till date. In the present work, we have put forth the idea of the selective design of potent and specific CDK inhibitor. The approach involved a comparative analysis of structural differences between several CDKs ATP binding site and their inhibitor specificity by depicting the principal ligand- CDK interactions for individual CDKs (Figure 23) to be targeted. The important find outs for CDK specific inhibitor design can be created by taking into consideration the amino acid residues changes, nature of amino acid(s) in the active site of CDK, conformational changes of the residues in active site, interacting residues, binding energy, and the properties like volume of ligand, volume of active site, remote cysteine residue for covalent inhibition, etc. These parameters have been briefly explained by taking an example in each case. Therefore, it is expected that the current findings would provide ample scope and opportunities to the medicinal and computational researchers to discover and design novel and selective CDK inhibitors as therapeutic strategies to treat various types of cancer.

ACCEPTED MANUSCRIPT

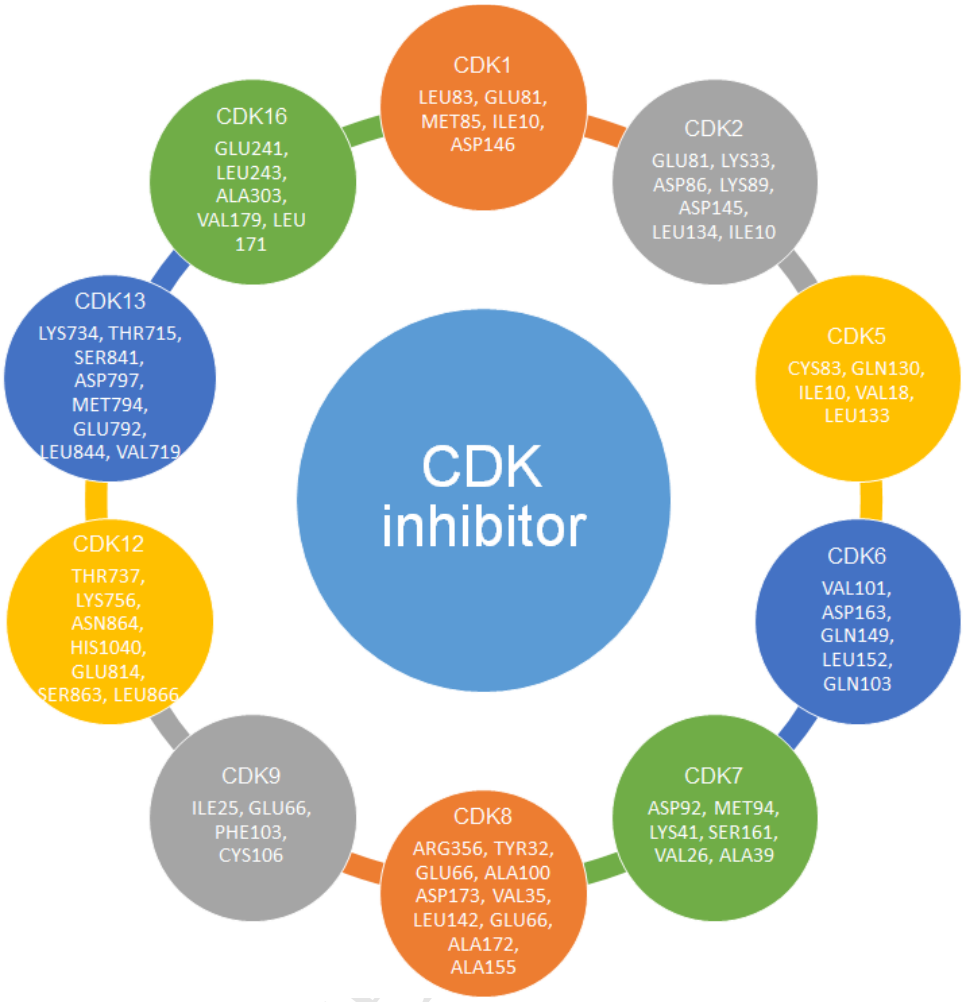

Figure 23. Conclusive representation of the interacting residues in the respective CDKs defining the criteria of an inhibitor to be a specific CDK inhibitor

Acknowledgement

AM and SK thank ICMR, New Delhi, India for the financial assistance BIC/12(32)/2012. SK is the recipient of JRF from the project. RK and GJ thank Bristol-Myer Squibb (Grant # 34003085), USA for financial support.

Conflict of interest

The authors declare no conflict of interest.

References

[1] D. Hanahan, R.A. Weinberg, Hallmarks of cancer: the next generation, Cell, 144 (2011) 646-674.

[2] D. Hanahan, R.A. Weinberg, The hallmarks of cancer, Cell, 100 (2000) 57-70.

[3] M. Chauhan, G. Joshi, H. Kler, A. Kashyap, S.M. Amrutkar, P. Sharma, K.D. Bhilare, U.C. Banerjee, S. Singh, R. Kumar, Dual inhibitors of epidermal growth factor receptor and topoisomerase IIα derived from a quinoline scaffold, RSC Adv., 6 (2016) 77717-77734.

[4] G. Joshi, P.K. Singh, A. Negi, A. Rana, S. Singh, R. Kumar, Growth factors mediated cell signalling in prostate cancer progression: implications in discovery of anti-prostate cancer agents, Chem. Biol. Interact., 240 (2015) 120-133.

[5] M. Malumbres, Cyclin-dependent kinases, Genome Biol., 15 (2014) 1 - 10.

[6] J. Harper, P. Adams, Cyclin-dependent kinases, Chem. Rev., 101 (2001) 2511-2526.

[7] J. Zhang, P.L. Yang, N.S. Gray, Targeting cancer with small molecule kinase inhibitors, Nat. Rev. Canc., 9 (2009) 28-39.

[8] E.A. Nigg, Cyclin-dependent protein kinases: key regulators of the eukaryotic cell cycle, Bioessays, 17 (1995) 471-480.

[9] H. Matsushime, D. Quelle, S. Shurtleff, M. Shibuya, C. Sherr, J. Kato, D-type cyclin-dependent kinase activity in mammalian cells, Mol. Cell. Biol., 14 (1994) 2066-2076.

[10] C. Giacinti, A. Giordano, RB and cell cycle progression, Oncogene, 25 (2006) 5220-5227.

[11] Y.-J. Chen, C. Dominguez-Brauer, Z. Wang, J.M. Asara, R.H. Costa, A.L. Tyner, L.F. Lau, P. Raychaudhuri, A conserved phosphorylation site within the forkhead domain of FoxM1B is required for its activation by cyclin-CDK1, J. Biol. Chem., 284 (2009) 30695-30707.

[12] A.A. Russo, P.D. Jeffrey, A.K. Patten, J. Massagué, N.P. Pavletich, Crystal structure of the p27Kip1 cyclin-dependent-kinase inibitor bound to the cyclin A-Cdk2 complex, Nature, 382 (1996) 325.

[13] A. Tomashevski, D. Webster, P. Grammas, M. Gorospe, I. Kruman, Cyclin C-dependent cell cycle entry is required for activation of nonhomologous end joining DNA repair in postmitotic neurons, Cell Death Differ., 17 (2010) 1189 - 1198.

[14] P. Aggarwal, L.P. Vaites, J.K. Kim, H. Mellert, B. Gurung, H. Nakagawa, M. Herlyn, X. Hua, A.K. Rustgi, S.B. McMahon, Nuclear cyclin D1/CDK4 kinase regulates CUL4 expression

and triggers neoplastic growth via activation of the PRMT5 methyltransferase, Cancer cell, 18 (2010) 329-340.

[15] G. Lavoie, Y. St-Pierre, Phosphorylation of human DNMT1: implication of cyclin-dependent kinases, Biochem. Biophys. Res. Commun., 409 (2011) 187-192.

[16] R.P. Fisher, D.O. Morgan, A novel cyclin associates with M015/CDK7 to form the CDK-activating kinase, Cell, 78 (1994) 713-724.

[17] R. Firestein, A.J. Bass, S.Y. Kim, I.F. Dunn, S.J. Silver, I. Guney, E. Freed, A.H. Ligon, N. Vena, S. Ogino, CDK8 is a colorectal cancer oncogene that regulates β-catenin activity, Nature, 455 (2008) 547-551.

[18] T. Dale, P.A. Clarke, C. Esdar, D. Waalboer, O. Adeniji-Popoola, M.-J. Ortiz-Ruiz, A. Mallinger, R.S. Samant, P. Czodrowski, D. Musil, A selective chemical probe for exploring the role of CDK8 and CDK19 in human disease, Nat. Chem. Biol., 11 (2015) 973 - 980.

[19] S.Y. David, R. Zhao, E.L. Hsu, J. Cayer, F. Ye, Y. Guo, Y. Shyr, D. Cortez, Cyclin-dependent kinase 9–cyclin K functions in the replication stress response, EMBO Rep., 11 (2010) 876-882.

[20] X.-y. Zhong, X.-x. Xu, J.-h. Yu, G.-x. Jiang, Y. Yu, S. Tai, Z.-d. Wang, Y.-f. Cui, Clinical and biological significance of Cdk10 in hepatocellular carcinoma, Gene, 498 (2012) 68-74.

[21] D. Hu, A. Mayeda, J.H. Trembley, J.M. Lahti, V.J. Kidd, CDK11 complexes promote pre-mRNA splicing, J. Biol. Chem., 278 (2003) 8623-8629.

[22] D. Blazek, J. Kohoutek, K. Bartholomeeusen, E. Johansen, P. Hulinkova, Z. Luo, P. Cimermancic, J. Ule, B.M. Peterlin, The Cyclin K/Cdk12 complex maintains genomic stability via regulation of expression of DNA damage response genes, Genes Dev., 25 (2011) 2158-2172.

[23] S.-W.G. Cheng, M.A. Kuzyk, A. Moradian, T.-A. Ichu, V.C.-D. Chang, J.F. Tien, S.E. Vollett, M. Griffith, M.A. Marra, G.B. Morin, Interaction of cyclin-dependent kinase 12/CrkRS with cyclin K1 is required for the phosphorylation of the C-terminal domain of RNA polymerase II, Mol. Cell. Biol., 32 (2012) 4691-4704.

[24] G. Davidson, The cell cycle and Wnt, in, Taylor & Francis, 2010, pp. 1667 - 1668.

[25] M.H. Park, S.Y. Kim, Y.J. Kim, Y.-H. Chung, ALS2CR7 (CDK15) attenuates TRAIL induced apoptosis by inducing phosphorylation of survivin Thr34, Biochem. Biophys. Res. Commun., 450 (2014) 129-134.

[26] P. Mikolcevic, R. Sigl, V. Rauch, M.W. Hess, K. Pfaller, M. Barisic, L.J. Pelliniemi, M. Boesl, S. Geley, Cyclin-dependent kinase 16/PCTAIRE kinase 1 is activated by cyclin Y and is essential for spermatogenesis, Mol. Cell. Biol., 32 (2012) 868-879.

[27] N.Y. Tan, L.M. Khachigian, Sp1 phosphorylation and its regulation of gene transcription, Mol. Cell. Biol., 29 (2009) 2483-2488.

[28] S. Matsuda, K. Kawamoto, K. Miyamoto, A. Tsuji, K. Yuasa, PCTK3/CDK18 regulates cell migration and adhesion by negatively modulating FAK activity, Sci. Rep., 7 (2017) 45545-45559.

[29] Y. Liu, C. Wu, K. Galaktionov, p42, a novel cyclin-dependent kinase-activating kinase in mammalian cells, J. Biol. Chem., 279 (2004) 4507-4514.

[30] W. Taylor, A. Grabovich, Targeting the cell cycle to kill cancer cells, Pharmacology: Principles and Practice. Academic Press, Burlington, MA, (2009) 429-453.

[31] H.L. Ford, A.B. Pardee, The S phase: beginning, middle, and end: a perspective, J. Cell. Biochem., 72 (1998) 1-7.

[32] A.S. Lundberg, R.A. Weinberg, Functional inactivation of the retinoblastoma protein requires sequential modification by at least two distinct cyclin-cdk complexes, Mol. Cell. Biol., 18 (1998) 753-761.

[33] C.J. Sherr, The Pezcoller lecture: cancer cell cycles revisited, Cancer Res., 60 (2000) 3689-3695.

[34] S. Mourón, G. de Cárcer, E. Seco, G. Fernández-Miranda, M. Malumbres, A.R. Nebreda, RINGO C is required to sustain the spindle-assembly checkpoint, J. Cell Sci., 123 (2010) 2586-2595.

[35] A.R. Nebreda, CDK activation by non-cyclin proteins, Curr. Opin. Cell Biol., 18 (2006) 192-198.

[36] A. Marais, Z. Ji, E.S. Child, E. Krause, D.J. Mann, A.D. Sharrocks, Cell cycle-dependent regulation of the forkhead transcription factor FOXK2 by CDK· cyclin complexes, J. Biol. Chem., 285 (2010) 35728-35739.

[37] X. Zhao, D. Feng, Q. Wang, A. Abdulla, X.-J. Xie, J. Zhou, Y. Sun, E.S. Yang, L.-P. Liu, B. Vaitheesvaran, Regulation of lipogenesis by cyclin-dependent kinase 8–mediated control of SREBP-1, J. Clin. Invest., 122 (2012) 2417-2427.

[38] F. Bienvenu, S. Jirawatnotai, J.E. Elias, C.A. Meyer, K. Mizeracka, A. Marson, G.M. Frampton, M.F. Cole, D.T. Odom, J. Odajima, Transcriptional role of cyclin D1 in development revealed by a genetic–proteomic screen, Nature, 463 (2010) 374-378.

[39] J. Odajima, Z.P. Wills, Y.M. Ndassa, M. Terunuma, K. Kretschmannova, T.Z. Deeb, Y. Geng, S. Gawrzak, I.M. Quadros, J. Newman, Cyclin E constrains Cdk5 activity to regulate synaptic plasticity and memory formation, Dev. Cell, 21 (2011) 655-668.

[40] B. Bartkowiak, P. Liu, H.P. Phatnani, N.J. Fuda, J.J. Cooper, D.H. Price, K. Adelman, J.T. Lis, A.L. Greenleaf, CDK12 is a transcription elongation-associated CTD kinase, the metazoan ortholog of yeast Ctk1, Genes Dev., 24 (2010) 2303-2316.

[41] S. Lim, P. Kaldis, Cdks, cyclins and CKIs: roles beyond cell cycle regulation, Development, 140 (2013) 3079-3093.

[42] G. Davidson, J. Shen, Y.-L. Huang, Y. Su, E. Karaulanov, K. Bartscherer, C. Hassler, P. Stannek, M. Boutros, C. Niehrs, Cell cycle control of wnt receptor activation, Dev. Cell, 17 (2009) 788-799.

[43] D.O. Morgan, The cell cycle: principles of control, New Science Press, 2007.

[44] S. Ortega, M. Malumbres, M. Barbacid, Cyclin D-dependent kinases, INK4 inhibitors and cancer, BBA Rev. on Cancer, 1602 (2002) 73-87.

[45] E.T. Cánepa, M.E. Scassa, J.M. Ceruti, M.C. Marazita, A.L. Carcagno, P.F. Sirkin, M.F. Ogara, INK4 proteins, a family of mammalian CDK inhibitors with novel biological functions, IUBMB life, 59 (2007) 419-426.

[46] M.F. Roussel, The INK4 family of cell cycle inhibitors in cancer, Oncogene, 18 (1999) 5311-5317.

[47] J. Wang, S. Liu, Y. Fu, J.H. Wang, Y. Lu, Cdk5 activation induces hippocampal CA1 cell death by directly phosphorylating NMDA receptors, Nat. Neurosci., 6 (2003) 1039-1047.

[48] L.M. Schang, Effects of pharmacological cyclin-dependent kinase inhibitors on viral transcription and replication, Biochim. Biophys. Acta-Proteins and Proteomics, 1697 (2004) 197-209.

[49] L.-H. Tsai, M.-S. Lee, J. Cruz, Cdk5, a therapeutic target for Alzheimer's disease?, Biochim. Biophys. Acta-Proteins and Proteomics, 1697 (2004) 137-142.

[50] P.D. Smith, M.J. O'Hare, D.S. Park, CDKs: taking on a role as mediators of dopaminergic loss in Parkinson's disease, Trends Mol. Med., 10 (2004) 445-451.

[51] P.D. Smith, S.J. Crocker, V. Jackson-Lewis, K.L. Jordan-Sciutto, S. Hayley, M.P. Mount, M.J. O'Hare, S. Callaghan, R.S. Slack, S. Przedborski, Cyclin-dependent kinase 5 is a mediator of dopaminergic neuron loss in a mouse model of Parkinson's disease, Proc. Natl. Acad. Sci., 100 (2003) 13650-13655.

[52] P.J. Nelson, S.J. Shankland, Therapeutics in renal disease: the road ahead for antiproliferative targets, Nephron Exp. Nephrol., 103 (2005) e6-e15.

[53] L. MEIJER, Pharmacological inhibitors of disease-relevant cyclin-dependent kinases.

[54] R. Roskoski, A historical overview of protein kinases and their targeted small molecule inhibitors, Pharmacol. Res., 100 (2015) 1-23.

[55] T. Li, T. Weng, M. Zuo, Z. Wei, M. Chen, Z. Li, Recent progress of cyclin-dependent kinase inhibitors as potential anticancer agents, Future Med. Chem., 8 (2016) 2047-2076.

[56] S. Betzi, R. Alam, M. Martin, D.J. Lubbers, H. Han, S.R. Jakkaraj, G.I. Georg, E. Schönbrunn, Discovery of a potential allosteric ligand binding site in CDK2, ACS Chem. Biol., 6 (2011) 492-501.

[57] G. Rastelli, A. Anighoro, M. Chripkova, L. Carrassa, M. Broggini, Structure-based discovery of the first allosteric inhibitors of cyclin-dependent kinase 2, Cell Cycle, 13 (2014) 2296-2305.

[58] U. Asghar, A.K. Witkiewicz, N.C. Turner, E.S. Knudsen, The history and future of targeting cyclin-dependent kinases in cancer therapy, Nat. Rev. Drug Discov., 14 (2015) 130 - 146.

[59] A. Besson, S.F. Dowdy, J.M. Roberts, CDK inhibitors: cell cycle regulators and beyond, Dev. Cell, 14 (2008) 159-169.

[60] C. Sánchez-Martínez, L.M. Gelbert, M.J. Lallena, A. de Dios, Cyclin dependent kinase (CDK) inhibitors as anticancer drugs, Bioorg. Med. Chem. Lett., 25 (2015) 3420-3435.

[61] T. Li, T. Weng, M. Zuo, Z. Wei, M. Chen, Z. Li, Recent progress of cyclin-dependent kinase inhibitors as potential anticancer agents, Future, 8 (2016) 2047-2076.

[62] N.R. Brown, S. Korolchuk, M.P. Martin, W.A. Stanley, R. Moukhametzianov, M.E. Noble, J.A. Endicott, CDK1 structures reveal conserved and unique features of the essential cell cycle CDK, Nat. Comm., 6 (2015) 6769 - 6780.

[63] D.M. Jacobsen, Z.-Q. Bao, P. O'Brien, C.L. Brooks III, M.A. Young, Price to be paid for two-metal catalysis: magnesium ions that accelerate chemistry unavoidably limit product release from a protein kinase, J. Am. Chem. Soc., 134 (2012) 15357-15370.

[64] P. Ayaz, D. Andres, D.A. Kwiatkowski, C.-C. Kolbe, P. Lienau, G. Siemeister, U. Lücking, C.M. Stegmann, Conformational Adaption May Explain the Slow Dissociation Kinetics of Roniciclib (BAY 1000394), a Type I CDK Inhibitor with Kinetic Selectivity for CDK2 and CDK9, ACS Chem. Biol., 11 (2016) 1710-1719.

[65] J.F. Blake, M. Burkard, J. Chan, H. Chen, K.-J. Chou, D. Diaz, D.A. Dudley, J.J. Gaudino, S.E. Gould, J. Grina, Discovery of (S)-1-(1-(4-Chloro-3-fluorophenyl)-2-hydroxyethyl)-4-(2-((1-methyl-1H-pyrazol-5-yl) amino) pyrimidin-4-yl) pyridin-2 (1H)-one (GDC-0994), an Extracellular Signal-Regulated Kinase 1/2 (ERK1/2) Inhibitor in Early Clinical Development, J. Med. Chem., 59 (2016) 5650-5660.

[66] P.J. Day, A. Cleasby, I.J. Tickle, M. O'Reilly, J.E. Coyle, F.P. Holding, R.L. McMenamin, J. Yon, R. Chopra, C. Lengauer, Crystal structure of human CDK4 in complex with a D-type cyclin, Proc. Natl. Acad. Sci., 106 (2009) 4166-4170.

[67] T. Takaki, A. Echalier, N. Brown, T. Hunt, J. Endicott, M. Noble, The structure of CDK4/cyclin D3 has implications for models of CDK activation, Proc. Natl. Acad. Sci., 106 (2009) 4171-4176.

[68] C. Tarricone, R. Dhavan, J. Peng, L.B. Areces, L.-H. Tsai, A. Musacchio, Structure and regulation of the CDK5-p25 nck5a complex, Mol. Cell, 8 (2001) 657-669.

[69] M. Mapelli, L. Massimiliano, C. Crovace, M.A. Seeliger, L.-H. Tsai, L. Meijer, A. Musacchio, Mechanism of CDK5/p25 binding by CDK inhibitors, J. Med. Chem., 48 (2005) 671-679.

[70] J.S. Ahn, M.L. Radhakrishnan, M. Mapelli, S. Choi, B. Tidor, G.D. Cuny, A. Musacchio, L.-A. Yeh, K.S. Kosik, Defining Cdk5 ligand chemical space with small molecule inhibitors of tau phosphorylation, Chem. Biol., 12 (2005) 811-823.

[71] J. Malmström, J. Viklund, C. Slivo, A. Costa, M. Maudet, C. Sandelin, G. Hiller, L.-L. Olsson, A. Aagaard, S. Geschwindner, Synthesis and structure-activity relationship of 4-(1, 3-benzothiazol-2-yl)-thiophene-2-sulfonamides as cyclin-dependent kinase 5 (cdk5)/p25 inhibitors, Bioorg. Med. Chem. Lett., 22 (2012) 5919-5923.

[72] H. Lu, D.J. Chang, B. Baratte, L. Meijer, U. Schulze-Gahmen, Crystal structure of a human cyclin-dependent kinase 6 complex with a flavonol inhibitor, fisetin, J. Med. Chem., 48 (2005) 737-743.

[73] H. Lu, U. Schulze-Gahmen, Toward understanding the structural basis of cyclin-dependent kinase 6 specific inhibition, J. Med. Chem., 49 (2006) 3826-3831.

[74] G. Lolli, E.D. Lowe, N.R. Brown, L.N. Johnson, The crystal structure of human CDK7 and its protein recognition properties, Structure, 12 (2004) 2067-2079.

[75] H.E. Pelish, B.B. Liau, I.I. Nitulescu, A. Tangpeerachaikul, Z.C. Poss, D.H. Da Silva, B.T. Caruso, A. Arefolov, O. Fadeyi, A.L. Christie, Mediator kinase inhibition further activates super-enhancer-associated genes in AML, Nature, 526 (2015) 273-276.

[76] E.V. Schneider, J. Böttcher, R. Huber, K. Maskos, L. Neumann, Structure–kinetic relationship study of CDK8/CycC specific compounds, Proc. Natl. Acad. Sci., 110 (2013) 8081-8086.

[77] S. Baumli, A.J. Hole, M.E. Noble, J.A. Endicott, The CDK9 C-helix exhibits conformational plasticity that may explain the selectivity of CAN508, ACS Chem. Biol., 7 (2012) 811-816.

[78] S. Baumli, J.A. Endicott, L.N. Johnson, Halogen bonds form the basis for selective P-TEFb inhibition by DRB, Chem. Biol., 17 (2010) 931-936.

[79] S. Baumli, G. Lolli, E.D. Lowe, S. Troiani, L. Rusconi, A.N. Bullock, J.É. Debreczeni, S. Knapp, L.N. Johnson, The structure of P-TEFb (CDK9/cyclin T1), its complex with flavopiridol and regulation by phosphorylation, EMBO J., 27 (2008) 1907-1918.

[80] K. Bettayeb, D. Baunbæk, C. Delehouze, N. Loaëc, A.J. Hole, S. Baumli, J.A. Endicott, S. Douc-Rasy, J. Bénard, N. Oumata, CDK inhibitors roscovitine and CR8 trigger Mcl-1 down-regulation and apoptotic cell death in neuroblastoma cells, Genes Cancer, 1 (2010) 369-380.

[81] S.E. Dixon-Clarke, J.M. Elkins, S.-W.G. Cheng, G.B. Morin, A.N. Bullock, Structures of the CDK12/CycK complex with AMP-PNP reveal a flexible C-terminal kinase extension important for ATP binding, Sci. Rep., 5 (2015) 17122 - 17134.

[82] C.A. Bösken, L. Farnung, C. Hintermair, M.M. Schachter, K. Vogel-Bachmayr, D. Blazek, K. Anand, R.P. Fisher, D. Eick, M. Geyer, The structure and substrate specificity of human Cdk12/Cyclin K, Nat. Comm., 5 (2014) 3505 - 3518.

[83] A.K. Greifenberg, D. Hönig, K. Pilarova, R. Düster, K. Bartholomeeusen, C.A. Bösken, K. Anand, D. Blazek, M. Geyer, Structural and Functional Analysis of the Cdk13/Cyclin K Complex, Cell Rep., 14 (2016) 320-331.

[84] M. Castedo, J.-L. Perfettini, T. Roumier, K. Andreau, R. Medema, G. Kroemer, Cell death by mitotic catastrophe: a molecular definition, Oncogene, 23 (2004) 2825-2837.

[85] P. Schrödinger, version 3.5, LLC, New York, NY, (2014).

[86] M.P. Jacobson, D.L. Pincus, C.S. Rapp, T.J. Day, B. Honig, D.E. Shaw, R.A. Friesner, A hierarchical approach to all-atom protein loop prediction, Proteins: Struct., Funct., Bioinf., 55 (2004) 351-367.

[87] M.P. Jacobson, R.A. Friesner, Z. Xiang, B. Honig, On the role of the crystal environment in determining protein side-chain conformations, J. Mol. Biol., 320 (2002) 597-608.

[88] D. Parry, T. Guzi, F. Shanahan, N. Davis, D. Prabhavalkar, D. Wiswell, W. Seghezzi, K. Paruch, M.P. Dwyer, R. Doll, Dinaciclib (SCH 727965), a novel and potent cyclin-dependent kinase inhibitor, Mol. Cancer Ther., 9 (2010) 2344-2353.

[89] N. Kwiatkowski, T. Zhang, P.B. Rahl, B.J. Abraham, J. Reddy, S.B. Ficarro, A. Dastur, A. Amzallag, S. Ramaswamy, B. Tesar, Targeting transcription regulation in cancer with a covalent CDK7 inhibitor, Nature, 511 (2014) 616 - 620.

[90] Z. Zhao, Q. Liu, S. Bliven, L. Xie, P.E. Bourne, Determining cysteines available for covalent inhibition across the human kinome, J. Med. Chem., 60 (2017) 2879-2889.

[91] T. Zhang, N. Kwiatkowski, C.M. Olson, S.E. Dixon-Clarke, B.J. Abraham, A.K. Greifenberg, S.B. Ficarro, J.M. Elkins, Y. Liang, N.M. Hannett, Covalent targeting of remote cysteine residues to develop CDK12 and 13 inhibitors, Nat. Chem. Biol., 12 (2016) 876 - 884.

[92] N.M. Mascarenhas, N. Ghoshal, Combined ligand and structure based approaches for narrowing on the essential physicochemical characteristics for CDK4 inhibition, J. Chem. Inf. Model., 48 (2008) 1325-1336.

[93] M.I. Shafiq, T. Steinbrecher, R. Schmid, Fascaplysin as a specific inhibitor for CDK4: Insights from molecular modelling, PLoS One, 7 (2012) e42612.

[94] P. Broto, G. Moreau, C. Vandycke, Molecular structures: perception, autocorrelation descriptor and SAR studies. Autocorrelation descriptor, Eur. J. Med. Chem., 19 (1984) 66-70.

[95] J. Gasteiger, J. Sadowski, J. Schuur, P. Selzer, L. Steinhauer, V. Steinhauer, Chemical information in 3D space, J. Chem. Inf. & Comp. Sci., 36 (1996) 1030-1037.

[96] R. Todeschini, P. Gramatica, 3D-modelling and prediction by WHIM descriptors. 6. Application of WHIM descriptors in QSAR studies, Quant. Struct.-Act. Relat., 16 (1997) 120-125.

[97] M. González, C. Terán, M. Teijeira, M. Gonzalez-Moa, GETAWAY descriptors to predicting A 2A adenosine receptors agonists, Eur. J. Med. Chem., 40 (2005) 1080-1086.

[98] C.W. Yap, PaDEL-descriptor: An open source software to calculate molecular descriptors and fingerprints, J. Comput. Chem., 32 (2011) 1466-1474.

[99] S. Kalra, A. Kumar, M.K. Gupta, Modeling of antitubercular activity of biphenyl analogs of 2-nitroimidazo [2, 1-b][1, 3] oxazine to rationalize their activity profile, Med. Chem. Res., 22 (2013) 3444-3451.

ACCEPTED MANUSCRIPT